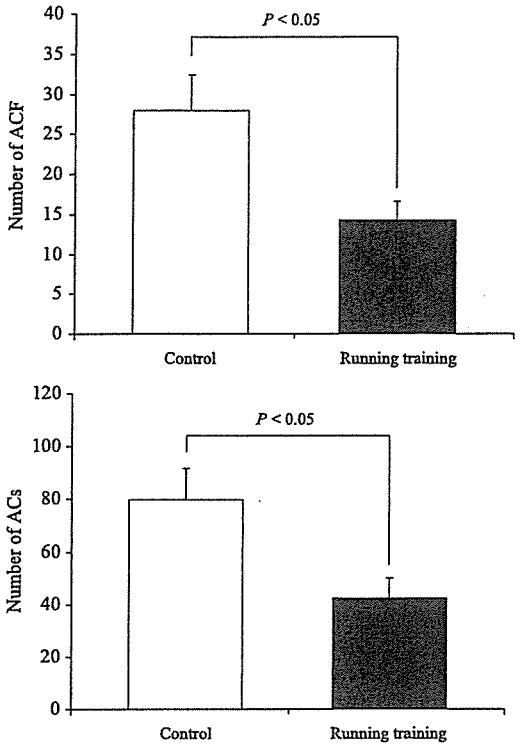

FIGURE 2—Effect of running training on the number of 1,2-dimethylhydrazine-induced ACF (*upper*) and AC (*lower*) in the rat colon. ACF, aberrant crypt foci; AC, aberrant crypts.

significantly less than that of the control rats ($P < 0.01$) (Table 1). The weight of heart and soleus, expressed relative to body weight, was significantly heavier in the training group compared with the control group ($P < 0.05$ and $P < 0.001$, respectively), whereas the relative adipose tissue weight of the peritoneum and epididymides was significantly lighter in the training group compared with the control group ($P < 0.001$ and $P < 0.05$, respectively).

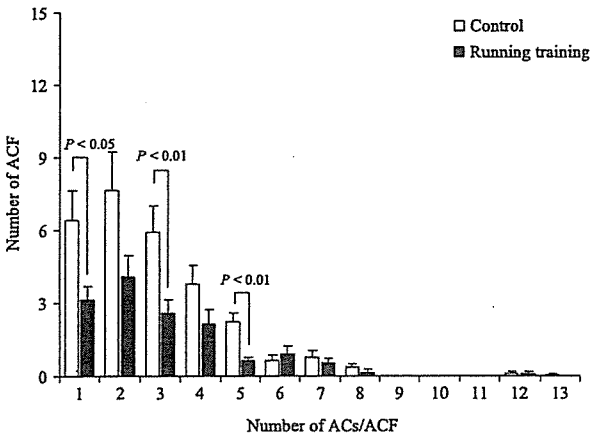

FIGURE 3—Effect of running training on the number of 1,2-dimethylhydrazine-induced AC per focus in the rat colon. ACF, aberrant crypt foci; AC, aberrant crypts.

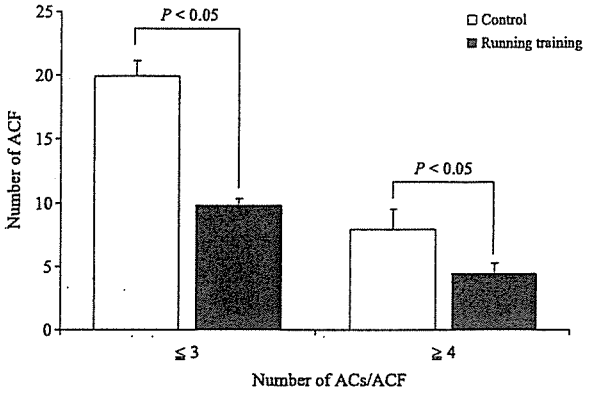

FIGURE 4—Effect of running training on the number of 1,2-dimethylhydrazine-induced small ACF (aberrant crypts per focus ≤ 3) and large ACF (aberrant crypts per focus ≥ 4) in the rat colon. ACF, aberrant crypt foci; AC, aberrant crypts.

The relative BAT weight of the training rats tended to be lower than that of the control group ($P = 0.07$). CS activity in the soleus muscle of the training group was significantly higher than in the control group ($P < 0.05$).

Induction of ACF and AC. As shown in Figure 2 upper panel, the number of ACF of training-group rats was significantly less than that observed in the control group ($P < 0.05$). The number of total AC was also significantly less in the training group than in the control group ($P < 0.05$; Fig. 2 lower panel). As shown in Figure 3, the occurrences of one, three, and five aberrant crypts per focus were significantly smaller in the training group than in the control group ($P < 0.05$). Furthermore, running training decreased the number of not only small ACF, which consists of less than or equal to three AC ($P < 0.05$), but also large ACF (≥ 4 AC) ($P < 0.05$), as compared with the control group (Fig. 4). However, the ratio of total AC/ACF, which indicates the average size of induced ACF, did not significantly differ between the training and control groups (2.9 ± 0.2 vs 2.9 ± 0.7, $P > 0.10$).

DISCUSSION

The main finding of the present study was that short-term, low-intensity running training reduced DMH-induced ACF production in the rat colon.

Colon carcinogenesis is well known to be a multistep process involving multiple genetic alterations (15,37,38). In humans, mutation of adenomatous polyposis coli (APC) gene is regarded as the initial event in ACF, followed by additional mutation of *K-ras* gene in adenomas; further mutation of the *p53* gene is the progressive event in carcinomas (14,33). In rodents, β-catenin mutations are frequently observed in colon tumors and in dysplastic ACF induced by azoxymethane (32). APC and/or K-ras mutations are also occasionally observed in rodents, as they are in humans (32), and ACF has been considered a very initial lesion in a

multistep colorectal tumorigenesis model (14). After ACF were first described in animals, similar lesions were found in humans (28). Because previous studies have suggested that low-intensity, long-term treadmill-running training prevented the incidence or development of colon tumors in a rat model injected subcutaneously with azoxymethane (36), it is reasonable to speculate that exercise training may exert its effect on one or more steps in colon carcinogenesis. To date, however, it remains unknown at which step of the carcinogenic process (e.g., ACF, adenomas (early, intermediate, and late), or carcinomas) physical exercise training exerts its preventive effect in rodents injected with carcinogens. The present results suggest that training in rats suppressed the first step, the initiation of ACF development in the rat colon. This is the first observation regarding the effect of physical exercise on ACF, the development of which is considered the first step in colon carcinogenesis. Furthermore, Colbert et al. (5), using the APC^{Min} mouse model, reported a trend toward fewer polyps in the colon in treadmill-exercised males compared with nonexercised mice. From the present investigation, it is obvious that the earlier phase of colon carcinogenesis is inhibited by exercise training. Therefore, it is of great importance when considering efficient chemopreventive effects on cancer development. Several hypotheses have been suggested to explain the preventive effects of exercise/physical activity on colon carcinogenesis—for example, shortened gastrointestinal transit time as a result of exercise (6); energy balance (16); reduced levels of blood insulin, which might be a growth factor for colon cancer cells (12); enhanced immune activity–related NK cells (20); enhanced free-radical scavenger system (8); changed prostaglandin levels (17); and decreased obesity (25). However, mechanisms related to the exercise-induced decrease in AC and/or ACF are not known at all. Therefore, only a few hypotheses can be raised. First, as Lasko and Bird et al. (16) have reported that caloric restriction–induced weight loss suppressed the increase in the number of ACF after the injection of azoxymethane in rats, it may be possible that energy balance (29), including energy expenditure and reduced food intake (24) or reduced nonexercise activity level (35) by exercise training, may exert a suppressive effect similar to that of caloric restriction, inhibiting the initiation or proliferation of ACF on the colonic mucosa. In fact, the results of the present study indicate that the body weight and/or adipose tissue weight of the peritoneum and epididymides were significantly lower in the running group than in the control group. Therefore, it is plausible that body- or fat weight loss yielded by physical exercise may reduce the initiation of ACF. Another plausible mechanism is that exercise might exhibit its preventive effects on mutation induction in the APC, *K-ras*, and/or *p53* genes through the induction of some detoxification enzymes for oxidative stresses. A third possibility is the commitment of moderate levels of physical exercise on the improvement of lipid metabolism. High fat levels in serum and low expression levels of lipid metabolism–related genes such as lipoprotein lipase in the liver and colon are now considered to have some significant impact on the development of intestinal tumors in the APC^{Min} mouse model (21,22). Further studies are expected to investigate the molecular mechanisms underlying exercise-induced effects on AC/ACF formation.

Recently, Demarzo and Garcia (7) reported that a single bout of exhaustive swimming exercise with a 2% weight tied to the tail was related to an elevated number of colonic ACF in untrained rats treated with DMH, when compared with a control group. Because this report included no description of the exercise protocol, such as a period of acclimatization that is usually given before acute bouts of exercise (27), it is not known how much "stress" was imposed on the exercised rats in the study. Therefore, we could not discuss the different effects of ACF production between the two studies in terms of exercise training–induced stress. On the other hand, the intensity of the swimming exercise with a 2% weight tied to the tail might be higher than that of the running training adopted in the present investigation. Thus, the exercise intensity may be a key factor determining the number of ACF after exercise. In fact, unaccustomed exhaustive and/or high-intensity exercise increases systemic free-radical generation in experimental animals (2). On the other hand, in the present study, we showed that low-intensity physical exercise for 2 h may decrease the development of colonic ACF in experimental animals. Furthermore, stress related to exercise at times during which the rats normally sleep may influence the ACF number in the colon. Therefore, voluntary exercise during the night cycle may be a better alternative exercise protocol than the "forced daytime" treadmill running adopted in the present investigation. However, because the number of ACF in the trained rats in the present study was actually lower than in the nonexercise control group, the overall effects of treadmill running on ACF production are favorable. Therefore, the benefits of the exercise training adopted in the present study are thought to outweigh the disadvantages of exercise-related stress. A future study using voluntary exercise should be conducted to clarify this issue.

The number of AC with a specific number of ACF (1,3,5) in the trained rats was lower than in the control group in the present investigation. However, running training did not affect the overall mean AC/ACF ratios of the rat colon induced by DMH. Thus, it is suggested that the physical exercise training adopted in the present investigation may not be effective for preventing the proliferation of ACF in rat colonic mucosa.

In conclusion, the results of the present investigation demonstrated that low-intensity running training inhibits the initiation of ACF in the rat colon induced by DMH. Furthermore, the present investigation suggests that increasing physical activity might be effective for primary prevention of colon cancer incidence, not only for rats but also for humans, by affecting the first step of cancer induction. However, the clinical implications and pathophysiological mechanisms of these findings warrant further investigation.

This work was supported in part by the Grants-in-Aid for Scientific Research on Exploratory Areas (16650160 to I.T.) from the Ministry of Education, Culture, Sports, Science and Technology, Japan, and by the Sasakawa Scientific Research Grant (to N.F.) from The Japan Science Society. The present addresses of Drs. N. Fuku and S. Terada are Division of Genomics for Longevity and Health, Tokyo Metropolitan Institute of Gerontology, Tokyo, Japan; and Washington University School of Medicine, St. Louis, MO, respectively.

REFERENCES

1. Andrianopoulos, G., R. L. Nelson, C. T. Bombeck, and G. Souza. The influence of physical activity in 1,2 dimethylhydrazine induced colon carcinogenesis in the rat. *Anticancer Res.* 7:849–852, 1987.
2. Banerjee, A. K., A. Mandal, D. Chanda, and S. Chakraborti. Oxidant, antioxidant and physical exercise. *Mol. Cell Biochem.* 253:307–312, 2003.
3. Bird, R. P. Observation and quantification of aberrant crypts in the murine colon treated with a colon carcinogen: preliminary findings. *Cancer Lett.* 37:147–151, 1987.
4. Bird, R. P. Role of aberrant crypt foci in understanding the pathogenesis of colon cancer. *Cancer Lett.* 93:55–71, 1995.
5. Colbert, L. H., J. M. Davis, D. A. Essig, A. Ghaffar, and E. P. Mayer. Exercise and tumor development in a mouse predisposed to multiple intestinal adenomas. *Med. Sci. Sports Exerc.* 32:1704–1708, 2000.
6. Cordain, L., R. W. Latin, and J. J. Behnke. The effects of an aerobic running program on bowel transit time. *J. Sports Med. Phys. Fitness* 26:101–104, 1986.
7. Demarzo, M. M., and S. B. Garcia. Exhaustive physical exercise increases the number of colonic preneoplastic lesions in untrained rats treated with a chemical carcinogen. *Cancer Lett.* 216:31–34, 2004.
8. Duthie, G. G., J. D. Robertson, R. J. Maughan, and P. C. Morrice. Blood antioxidant status and erythrocyte lipid peroxidation following distance running. *Arch. Biochem. Biophys.* 282:78–83, 1990.
9. Esteller, M., P. G. Corn, S. B. Baylin, and J. G. Herman. A gene hypermethylation profile of human cancer. *Cancer Res.* 61:3225–3229, 2001.
10. Fenoglio-Preiser, C. M., and A. Noffsinger. Aberrant crypt foci: a review. *Toxicol. Pathol.* 27:632–642, 1999.
11. Friedenreich, C. M., and M. R. Orenstein. Physical activity and cancer prevention: etiologic evidence and biological mechanisms. *J. Nutr.* 132:3456S–3464S, 2002.
12. Giovannucci, E. Insulin and colon cancer. *Cancer Causes Control* 6:164–179, 1995.
13. Kato, I., S. Tominaga, and A. Ikari. A case-control study of male colorectal cancer in Aichi Prefecture, Japan: with special reference to occupational activity level, drinking habits and family history. *Jpn. J. Cancer Res.* 81:115–121, 1990.
14. Kinzler, K. W., and B. Vogelstein. Lessons from hereditary colorectal cancer. *Cell* 87:159–170, 1996.
15. Kountouras, J., P. Boura, and N. J. Lygidakis. New concepts of molecular biology for colon carcinogenesis. *Hepatogastroenterology* 47:1291–1297, 2000.
16. Lasko, C. M., and R. P. Bird. Modulation of aberrant crypt foci by dietary fat and caloric restriction: the effects of delayed intervention. *Cancer Epidemiol. Biomarkers Prev.* 4:49–55, 1995.
17. Martinez, M. E., D. Heddens, D. L. Earnest, et al. Physical activity, body mass index, and prostaglandin E2 levels in rectal mucosa. *J. Natl. Cancer Inst.* 91:950–953, 1999.
18. McLellan, E. A., A. Medline, and R. P. Bird. Sequential analyses of the growth and morphological characteristics of aberrant crypt foci: putative preneoplastic lesions. *Cancer Res.* 51:5270–5274, 1991.
19. Nagao, M., T. Ushijima, M. Toyota, R. Inoue, and T. Sugimura. Genetic changes induced by heterocyclic amines. *Mutat. Res.* 376:161–167, 1997.
20. Nieman, D. C., S. L. Neilsen-Cannarella, P. A. Markoff, et al. The effects of moderate exercise training on natural killer cells and acute upper respiratory tract infections. *Int. J. Sports Med.* 11:467–473, 1990.
21. Niho, N., M. Mutoh, M. Takahashi, K. Tsutsumi, T. Sugimura, and K. Wakabayashi. Concurrent suppression of hyperlipidemia and intestinal polyp formation by NO-1886, increasing lipoprotein lipase activity in Min mice. *Proc. Natl. Acad. Sci. USA* 102:2970–2974, 2005.
22. Niho, N., M. Takahashi, T. Kitamura, et al. Concomitant suppression of hyperlipidemia and intestinal polyp formation in Apc-deficient mice by peroxisome proliferator-activated receptor ligands. *Cancer Res.* 63:6090–6095, 2003.
23. Ochiai, M., M. Ushigome, K. Fujiwara, et al. Characterization of dysplastic aberrant crypt foci in the rat colon induced by 2-amino-1-methyl-6-phenylimidazo[4,5-b]pyridine. *Am. J. Pathol.* 163:1607–1614, 2003.
24. Oscai, L. B., and J. O. Holloszy. Effects of weight changes produced by exercise, food restriction, or overeating on body composition. *J. Clin. Invest.* 48:2124–2128, 1969.
25. Parker, E. D., and A. R. Folsom. Intentional weight loss and incidence of obesity-related cancers: the Iowa Women's Health Study. *Int. J. Obes. Relat. Metab. Disord.* 27:1447–1452, 2003.
26. Reddy, B. S., S. Sugie, and A. Lowenfels. Effect of voluntary exercise on azoxymethane-induced colon carcinogenesis in male F344 rats. *Cancer Res.* 48:7079–7081, 1988.
27. Ren, J. M., C. F. Semenkovich, E. A. Gulve, J. Gao, and J. O. Holloszy. Exercise induces rapid increases in GLUT4 expression, glucose transport capacity, and insulin-stimulated glycogen storage in muscle. *J. Biol. Chem.* 269:14396–14401, 1994.
28. Roncucci, L., D. Stamp, A. Medline, J. B. Cullen, and W. R. Bruce. Identification and quantification of aberrant crypt foci and microadenomas in the human colon. *Hum. Pathol.* 22:287–294, 1991.
29. Slattery, M. L., M. Murtaugh, B. Caan, K. N. Ma, S. Neuhausen, and W. Samowitz. Energy balance, insulin-related genes and risk of colon and rectal cancer. *Int. J. Cancer* 115: 148–154, 2005.
30. Slattery, M. L., and J. D. Potter. Physical activity and colon cancer: confounding or interaction? *Med. Sci. Sports Exerc.* 34: 913–919, 2002.
31. Srere, P. Citrate synthase. *Method Enzymol.* 13:3–5, 1969.
32. Takahashi, M., and K. Wakabayashi. Gene mutations and altered gene expression in azoxymethane-induced colon carcinogenesis in rodents. *Cancer Sci.* 95:475–480, 2004.
33. Takayama, T., M. Ohi, T. Hayashi, et al. Analysis of K-ras, APC, and beta-catenin in aberrant crypt foci in sporadic adenoma, cancer, and familial adenomatous polyposis. *Gastroenterology* 121:599–611, 2001.
34. Terada, S., and I. Tabata. Effects of acute bouts of running and swimming exercise on PGC-1alpha protein expression in rat epitrochlearis and soleus muscle. *Am. J. Physiol. Endocrinol. Metab.* 286:E208–E216, 2004.
35. Thomas, B. M., and A. T. J. Miller. Adaptation to forced exercise in the rat. *Am. J. Physiol.* 193:350–354, 1958.
36. Thorling, E. B., N. O. Jacobsen, and K. Overvad. Effect of exercise on intestinal tumour development in the male Fischer rat after exposure to azoxymethane. *Eur. J. Cancer Prev.* 2:77–82, 1993.
37. Vogelstein, B., E. R. Fearon, S. R. Hamilton, et al. Genetic alterations during colorectal-tumor development. *N. Engl. J. Med.* 319:525–532, 1988.
38. Vogelstein, B., and K. W. Kinzler. The multistep nature of cancer. *Trends Genet.* 9:138–141, 1993.

Pathology International 2006; **56**: 490–493 doi:10.1111/j.1440-1827.2006.01996.x

Rapid Communication

Repeated fluorescence *in situ* hybridization by a microwave-enhanced protocol

Yasuhiko Kitayama,[1,2] Hisaki Igarashi,[1] Taeko Kozu,[1] Kiyoko Nagura,[1] Yohei Ohashi[2] and Haruhiko Sugimura[1]

[1]*First Department of Pathology, Hamamatsu University School of Medicine, Hamamatsu and* [2]*Department of Pathology, Shizuoka Saiseikai General Hospital, Shizuoka, Japan*

A novel re-hybridization protocol for pathology archive sections that uses microwave-assisted fluorescence *in situ* hybridization (FISH) is described. Stripping the probe from the pathology archive sections with HCl and re-hybridizing with the next probe by intermittent microwave irradiation generated clear signals without background noise. Repeated stripping and hybridization with numerous bacterial artificial chromosome (BAC)-derived probes would identify the profile of genome-wide changes in small lesions on sections.

Key words: chromosome instability, FISH, pathology archives, re-hybridization

DNA-DNA or DNA-RNA hybridization is one of the basic principles in molecular biology, and frequently used procedures such as Southern blotting and northern blotting take advantage of it.[1] In these procedures, we often reuse the membrane that DNA or RNA were transferred to and hybridized with probes, by stripping the probes and re-hybridizing with another probe. Fluorescence *in situ* hybridization (FISH) is a technique based on the principle of the stringent DNA-DNA, DNA-RNA, and RNA-RNA hybridization that is widely used to localize a specific sequence on the chromosomes or tissue specimens,[2] but there have been few reports on the procedures for serially stripping and re-hybridizing multiple DNA probes on the tissues.[3,4] We recently modified the FISH method[5] by using initial intermittent microwave (MW) irradiation to hybridize paraffin sections,[6] and obtained reproducible chromosomes signals in the interphase of cells in pathology archives, with good preservation of histological structure.[7] This modified method provided new genetic information on various human cancers stored in clinical settings,[5,8–10] but on many occasions we found that only a few slides are available in laboratory settings. In this communication we report stripping by HCl treatment and re-hybridization of DNA probes on tissue sections by a MW-assisted FISH protocol. We prepared different DNA probes hybridized with the corresponding genomic sequences in a single section cut from the formalin-fixed paraffin-embedded tissue. This new tip incorporating MW-assisted prehybridization, hybridization, and re-hybridization for tissue sections will enable sequential FISH on pathology archive sections and allow a great deal of information on various chromosomes or gene abnormalities to be obtained from just a few slides.

Correspondence: Haruhiko Sugimura, MD, First Department of Pathology, Hamamatsu University School of Medicine, 1-20-1 Handayama, Hamamatsu 431-3192, Japan. Email: hsugimur@hama-med.ac.jp

Received 20 March 2006. Accepted for publication 17 May 2006.

MATERIALS AND METHODS

Tissue samples were obtained from biopsy or surgical specimens of solid tumors fixed in a 4% neutral buffer of formaldehyde at room temperature for a few days, and embedded in paraffin by the routine method. Tissue sections (5 μm thick) had been prepared and first analyzed by the modified FISH technique previously described.[11,12] A panel of centromeric DNA probes and locus-specific identifier probes was purchased from Vysis (Downers Grove, IL, USA). All of the probes had been labeled with spectrum green or orange by nick translation. The sections were dewaxed by five successive 3 min washes in xylene, followed by five washes in ethanol. The sections in 0.01 mol/L citrate buffer (pH 6.0) were subjected to MW treatment for 10 min. After exposure to 0.2% pepsin/0.01 N HCl for 10 min at 37°C, the samples were aged for 10 min in 0.1% NP-40/2 × sodium chloride–sodium citrate buffer (SSC) for 10 min at 37°C, and their DNA was denatured in 70% formamide/2x SCC for 5 min at 85°C. A total of 10 μL of probe solution (hybridization buffer 7 μL, probe 1 μL, distilled water 2 μL) was then placed on a glass slide, and a coverslip was placed on it. This sample slide was

put into a MW processor (MI-77; Azumaya, Tokyo, Japan). The sample was subjected to intermittent MW irradiation (2.45 GHz, 300 W, 3 s on and 2 s off, 42°C). The MW irradiation should be performed for the first hour of a 4 h period of hybridization. 4,6-Diamidino-2-phenylindole (DAPI-I, 125 ng/mL; Vysis) was used for nuclear counterstaining. The sample was promptly examined with a fluorescence microscope (BX-51, Olympus, Tokyo, Japan) equipped with epifluorescence filters and a photometric CCD camera (Sensicam, Tokyo Instruments, Tokyo, Japan) on a stage with a computerized stage control system (MJ-PBX, MJ Mechax Company, Shizuoka, Japan). The images captured were digitized and stored in the image analysis software (IP Laboratory; Scanalytics, Fairfax, VA, USA). The second FISH procedure began with removal of DAPI-I staining with 2x SCC, that is, rinsing the slides in a vat containing 2x SCC several times. The initial FISH signal was then stripped by washing with 0.1 N HCl for 10 min at room temperature. After confirming disappearance of the initial signals, the slide was also washed with PBS and distilled water and treated with ethanol. A 10 μL mixed hybridization solution containing the second DNA probe was placed on the same slide glass with a coverslip. The slide was then put into the MW processor. The MW-assisted prehybridization (initial intermittent MW irradiation for hybridization) during the first hour of *in situ* hybridization (ISH, total time, 4 h) was performed as per the first FISH step. After nuclear counterstaining with DAPI-I, the sample was examined again. The microscopic image field was automatically adjusted by the computerized stage control system (MJ-PBX) to the field in which the first FISH signal had been observed. The signal images in the same cell nuclei in the second analysis were also captured and stored. The third FISH analysis with another probe on the same tissue section was performed in the same way. This method of perpetual FISH would allow us to carry out repeated analysis of a single tissue section using different DNA probes. The principle is shown in Fig. 1 and a flow chart is given in Table 1.

The cytology specimens, that is, smears and touch sections, were fixed with methanol/acetic acid and the DNA was denatured at 75°C for 2 min. After rinsing with ethanol five times, a 10 μL mixed hybridization solution with probe was placed on a specimen on a slide glass with a coverslip on it. The MW-assisted prehybridization step for 30 min, ISH for 3 h, and nuclear counterstaining was then performed in the same manner as aforementioned. The section was examined under a light microscope, and the images were stored on disk. The second FISH procedure started with removal of the coverslip and washing out of the signals with 0.1 N HCl for 30 min. After the second probe-mixed solution was placed on the specimen, the section was again subjected to MW-assisted hybridization under the same conditions as the first FISH analysis, except that denaturation and protease treatment were skipped.

Table 1 Re-FISH procedure

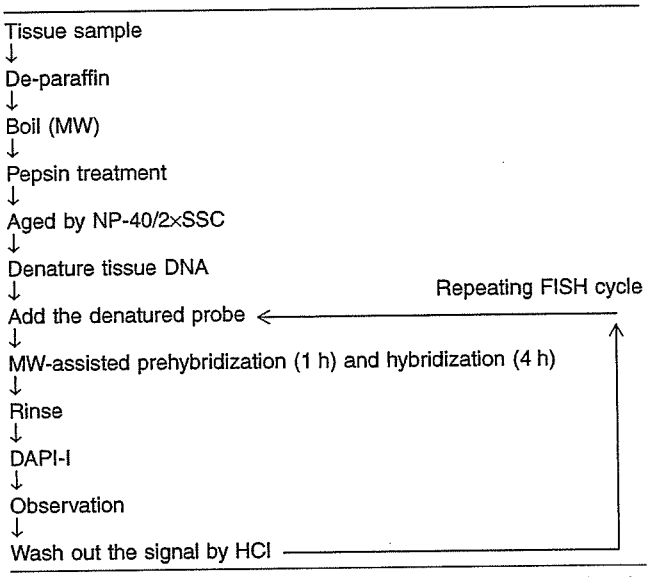

DAPI-I, 4,6-diamidino-2-phenylindole; FISH, fluorescence *in situ* hybridization; MW, microwave; SSC, sodium chloride–sodium citrate buffer.

RESULTS AND DISCUSSION

An example of re-FISH of a pathology archive section is shown in Fig. 2. The initial FISH analysis revealed a distinct signal of the centromere of chromosome 11 in a formalin-fixed paraffin-embedded section of gastric cancer (Fig. 2a). The second FISH, with CEP17, showed three and more signals of chromosome 17 in the same tumor cells on the same section as the first FISH analysis (Fig. 2b), and the centromeres of chromosome 18 were clearly detected on the same section by the third FISH and the centromeres of chromosome 9 by the fourth (Fig. 2c,d). The initial or residual signal on the section had disappeared each time after HCl treatment. Figure 3 shows a synthesized virtual color image of these four FISH reactions composed of the signals of chromosome 11 (yellow), chromosome 17 (red), chromosome 18 (green), and chromosome 9 (blue). The yellow signal looked amplified; there were two or three blue signals per cell, and the green and the red ones were almost disomies. The nuclear morphology of each tumor cell and the architecture of tumor were maintained even after several HCl treatments and MW irradiations. Background noise, debris, and crush artifacts are minimal with this procedure.

Since the genome-wide approach became available, pathologists have often been requested to detect multiple genetic changes in a single or few section slides. There are occasions when the tumor DNA changes revealed by the other methods such as comparative genomic hybridization (CGH) should be validated by FISH. Although bacterial artificial chromosome (BAC) probes are available for any locus

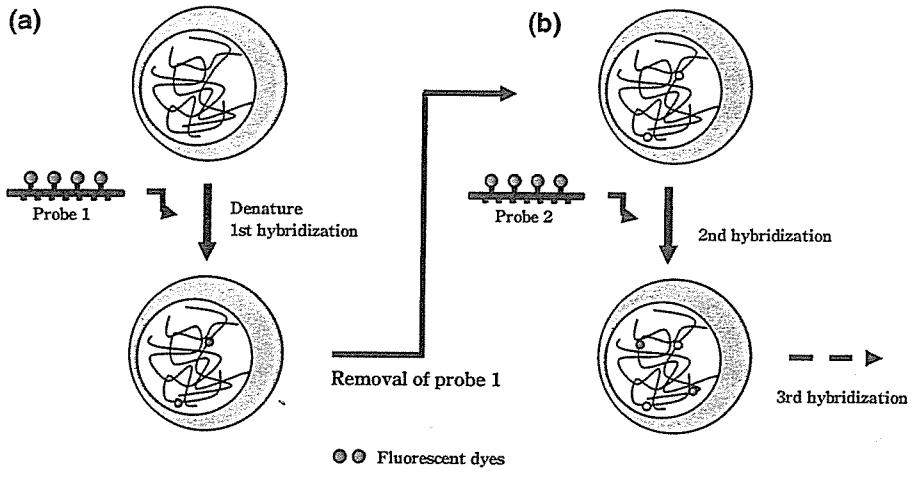

Figure 1 Schematic diagram of our (**a**) fluorescence *in situ* hybridization (FISH) and (**b**) repeating FISH procedure. (**a**) The first step consists of microwave (MW)-assisted FISH in interphase nuclei. (**b**) After removal of the first probe, the second FISH was performed with a different DNA probe.

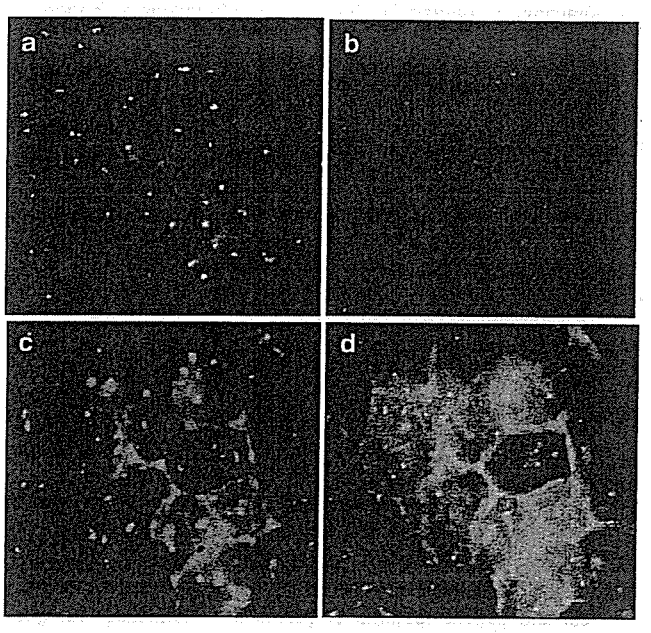

Figure 2 Example of re-fluorescence *in situ* hybridization (FISH) signals on the pathology archive slides. (**a**) Interphase nuclei of cancer cells were hybridized with labeled centromere chromosome 11 probe (CEP 11) by the first FISH. (**b**) In the second FISH, two or more chromosome 17 (CEP 17) signals were detected. (**c**) Similarly, three or more distinct signals were detected by the third (chromosome 18; CEP 18) and (**d**) fourth FISH step (chromosome 9; CEP9) on the same section.

Figure 3 Merged fluorescence *in situ* hybridization (FISH) image of the signals of chromosome 11 (yellow), chromosome 17 (red), chromosome 18 (green) and chromosome 9 (blue). This experiment consisted of four cycles of the re-FISH protocol described here.

in the genome, often only a few sections are available for analysis. Our modification of the FISH protocol for use in pathology archives was found to be versatile for re-probing on paraffin sections. Muller *et al.* reported four consecutive hybridization strategies for metaphase chromosomes.[3] They removed the probe simply by rinsing with 4x SSC/0.2% Tween and continued to hybridize with differently colored probes without confirming complete removal. They performed consecutive hybridizations with 24 colors to obtain 3-D images of interphase cells. They stated that their method was helpful for the study of chromosome territory of the cell nuclei. Our method includes the removal of the previous probes, which allowed the procedure to be repeated indefinitely. Eckel *et al.* followed the Muller *et al.* procedures and performed consecutive FISH on human oocytes in metaphase.[13] They fixed their specimen with methanol/acetone between the two adjacent rounds of hybridization to obtain the metaphase spread.

MW-assisted FISH had been successful in detecting abnormal chromosomal numbers in the interphase of tumor cells and precancerous lesions, which were often very small, <0.5 cm in diameter and consisted of tens of abnormal clusters of tumor cells.[14] We do not have any exact rationale to explain why MW treatment promotes DNA-DNA hybridization in formalin-fixed specimens, although several hypotheses have been proposed.[15,16] In any event, it worked well for re-FISH and sequential FISH procedures. The computerized stage control system for fluorescence microscopy was very

useful for re-FISH analysis, especially when we had to identify a few cell areas in a dark-field section.

Therefore, we now have the opportunity to test as many BAC probes as we choose, on a very small number of tissue sections.[14,17,18]

ACKNOWLEDGMENTS

This work was supported in part by a Grant-in-Aid from the Ministry of Health, Labor and Welfare for the 2nd-and 3rd-term Comprehensive 10-Year Strategy for Cancer Control (15–22), from the Smoking Research Foundation, and from the Ministry of Education, Culture, Sports, Science and Technology of Japan for Scientific Research (15290125) on Priority Area (17015017, 18014009) and the 21st century COE program Medical Photonics (Hamamatsu University School of Medicine), and by a Grant-in-Aid from the Foundation for Promotion of Cancer Research (HS).

REFERENCES

1 Sambrook J, Russel D. *Molecular Cloning: A Laboratory Manual*, **Vol. 1**, 3rd edn. Cold Spring Harbor: Cold Spring Harbor Laboratory Press, 2001.
2 Pinkel D, Gray JW, Trask B, van den Engh G, Fuscoe J, van Dekken H. Cytogenetic analysis by in situ hybridization with fluorescently labeled nucleic acid probes. *Cold Spring Harb Symp Quant Biol* 1986; **51 Part 1**: 151–7.
3 Muller S, Neusser M, Wienberg J. Towards unlimited colors for fluorescence in-situ hybridization (FISH). *Chromosome Res* 2002; **10**: 223–32.
4 Zhen DK, Wang JY, Falco VM, Weber W, Delli-Bovi L, Bianchi DW. Poly-FISH: A technique of repeated hybridizations that improves cytogenetic analysis of fetal cells in maternal blood. *Prenat Diagn* 1998; **18**: 1181–5.
5 Kitayama Y, Igarashi H, Sugimura H. Different vulnerability among chromosomes to numerical instability in gastric carcinogenesis: Stage-dependent analysis by FISH with the use of microwave irradiation. *Clin Cancer Res* 2000; **6**: 3139–46.
6 Kitayama Y, Igarashi H, Sugimura H. Amplification of FISH signals using intermittent microwave irradiation for analysis of chromosomal instability in gastric cancer. *Mol Pathol* 1999; **52**: 357–9.
7 Kitayama Y, Igarashi H, Sugimura H. Initial intermittent microwave irradiation for fluorescence in situ hybridization analysis in paraffin-embedded tissue sections of gastrointestinal neoplasia. *Lab Invest* 2000; **80**: 779–81.
8 Kobayashi K, Kitayama Y, Igarashi H *et al.* Intratumor heterogeneity of centromere numerical abnormality in multiple primary gastric cancers: Application of fluorescence in situ hybridization with intermittent microwave irradiation on paraffin-embedded tissue. *Jpn J Cancer Res* 2000; **91**: 1134–41.
9 Song JP, Kitayama Y, Igarashi H *et al.* Centromere numerical abnormality in the papillary, papillotubular type of early gastric cancer, a further characterization of a subset of gastric cancer. *Int J Oncol* 2002; **21**: 1205–11.
10 Nakamura R, Song JP, Isogaki J, Kitayama Y, Sugimura H. Multiple (multicentric and multifocal) cancers in the ipsilateral breast with different histologies: Profiles of chromosomal numerical abnormality. *Jpn J Clin Oncol* 2003; **33**: 463–9.
11 Kitayama Y, Igarashi H, Watanabe F, Maruyama Y, Kanamori M, Sugimura H. Nonrandom chromosomal numerical abnormality predicting prognosis of gastric cancer: A retrospective study of 51 cases using pathology archives. *Lab Invest* 2003; **83**: 1311–20.
12 Igarashi H, Yamashita K, Suzuki M *et al.* Simultaneous imaging of membrane antigen and the corresponding chromosomal locus in pathology archives. *Pathol Int* 2005; **55**: 753–6.
13 Eckel H, Kleinstein J, Wieacker P, Stumm M. Multi-locus (ML)-FISH is a reliable tool for nondisjunction studies in human oocytes. *Cytogenet Genome Res* 2003; **103**: 47–53.
14 Sano T, Kitayama Y, Igarashi H *et al.* Chromosomal numerical abnormalities in early stage lung adenocarcinoma. *Pathol Int* 2006; **56**: 117–25.
15 Lan HY, Mu W, Ng YY, Nikolic-Paterson DJ, Atkins RC. A simple, reliable, and sensitive method for nonradioactive in situ hybridization: Use of microwave heating to improve hybridization efficiency and preserve tissue morphology. *J Histochem Cytochem* 1996; **44**: 281–7.
16 Sibony M, Commo F, Callard P, Gasc JM. Enhancement of mRNA in situ hybridization signal by microwave heating. *Lab Invest* 1995; **73**: 586–91.
17 Kikuchi H, Yamashita K, Kawabata T *et al.* Immunohistochemical and genetic features of gastric and metastatic liver gastrointestinal stromal tumors: Sequential analyses. *Cancer Sci* 2006; **97**: 127–32.
18 Yamashita K, Igarashi H, Kitayama Y *et al.* Chromosomal numerical abnormality profiles of gastrointestinal stromal tumors. *Jpn J Clin Oncol* 2006; **36**: 85–92.

Oncogene (2006) 25, 5581–5590

www.nature.com/onc

ONCOGENOMICS

Molecular karyotyping of human hepatocellular carcinoma using single-nucleotide polymorphism arrays

Y Midorikawa[1,3,5], S Yamamoto[1,5], S Ishikawa[1], N Kamimura[1], H Igarashi[2], H Sugimura[2], M Makuuchi[3] and H Aburatani[1,4]

[1]Genome Science Division, Research Center for Advanced Science and Technology, The University of Tokyo, Tokyo, Japan; [2]1st Department of Pathology, Hamamatsu University School of Medicine, Shizuoka, Japan; [3]Hepato-Biliary-Pancreatic Surgery Division, The University of Tokyo, Tokyo, Japan and [4]Core Research for Evolutional Research and Technology; Japan Science and Technology agency, Saitama, Japan

Genomic amplification of oncogenes and inactivation of suppressor genes are critical in the pathogenesis of human cancer. To identify chromosomal alterations associated with hepatocarcinogenesis, we performed allelic gene dosage analysis on 36 hepatocellular carcinomas (HCCs). Data from high-density single-nucleotide polymorphism arrays were analysed using the Genome Imbalance Map (GIM) algorithm, which simultaneously detects DNA copy number alterations and loss of heterozygosity (LOH) events. Genome Imbalance Map analysis identified allelic imbalance regions, including uniparental disomy, and predicted the coexistence of a heterozygous population of cancer cells. We observed that gains of 1q, 5p, 5q, 6p, 7q, 8q, 17q and 20q, and LOH of 1p, 4q, 6q, 8p, 10q, 13q, 16p, 16q and 17p were significantly associated with HCC. On 6q24–25, which contains imprinting gene clusters, we observed reduced levels of *PLAGL1* expression owing to loss of the unmethylated allele. Finally, we integrated the copy number data with gene expression intensity, and found that genome dosage is correlated with alteration in gene expression. These observations indicated that high-resolution GIM analysis can accurately determine the localizations of genomic regions with allelic imbalance, and when integrated with epigenetic information, a mechanistic basis for inactivation of a tumor suppressor gene in HCC was elucidated.
Oncogene (2006) **25,** 5581–5590. doi:10.1038/sj.onc.1209537; published online 19 June 2006

Keywords: liver cancer; oligonucleotide array; SNP; allelic imbalance; copy number

Correspondence: Dr H Aburatani, Genome Science Division, Research Center for Advanced Science and Technology, The University of Tokyo, 4-6-1 Komaba, Meguro-ku, Tokyo 153-8904, Japan.
E-mail: haburata-tky@umin.ac.jp
[5]These contributed equally to this work.
Received 11 November 2005; revised 26 January 2006; accepted 15 February 2006; published online 19 June 2006

Introduction

Genomic amplification of oncogenes and inactivation of tumor suppressor genes are frequently associated with carcinogenesis. Comparative genomic hybridization (CGH) has been used extensively to detect genome-wide copy number changes in various types of cancers and to determine the localization of expression of many oncogenes and tumor suppressor genes (Kallioniemi *et al.*, 1992). Owing to its low resolution (greater than 20 Mb), CGH has not been useful in identifying micro-deletions or -amplifications. Array-based CGH using genomic DNA or cDNA clones has been developed to achieve higher resolution (Pinkel *et al.*, 1998; Pollack *et al.*, 1999). Furthermore, Lucito *et al.* (2003) have developed a new methodology, called ROMA (representational oligonucleotide microarray analysis), which achieves this purpose with an average resolution of 30 kb throughout the genome.

Despite the improvement in resolution, array-based CGH and high-density oligonucleotide arrays used for ROMA could only detect changes at the gene level and not at the level of individual alleles. Allelic changes, including hemizygous deletion with a gain of the opposite allele, so-called uniparental disomy (UPD) or trisomy (UPT), are important in elucidating the molecular mechanisms of cancer (Engel, 1980). For example, accurate determination of the copy number of each allele separately in the UPD region, which may contain a region of methylation or null mutation of tumor suppressor genes, may allow the mechanism of carcinogenesis to be determined more clearly and comprehensively (Grundy *et al.*, 1994; Murthy *et al.*, 2002; Raghavan *et al.*, 2005). In addition, accurate measurement of changes in copy number using high-resolution methods will help in the detection of heterogeneous populations among cancer cells (Benetkiewicz *et al.*, 2005; Buckley *et al.*, 2005).

Loss of heterozygosity (LOH) status can be analysed comprehensively by allelotyping of the genomic DNA from cancer cells using hundreds of polymorphic markers from each chromosomal arm (Weissenbach *et al.*, 1992). Polymerase chain reaction (PCR)-based measurement of simple sequence length polymorphisms

is a reliable method for detecting LOH, but is both expensive and labor intensive. Recently, global and high-resolution analyses of LOH using single-nucleotide polymorphism (SNP) arrays, which was originally designed for high-throughput SNP analysis (Wang *et al.*, 1998; Kennedy *et al.*, 2003), have been performed in various cancers (Lindblad-Toh *et al.*, 2000; Mei *et al.*, 2000; Lieberfarb *et al.*, 2003; Janne *et al.*, 2004). Comparing this method to PCR-based microsatellite analysis directly, Hoque *et al.* (2003) validated the accuracy of LOH analysis using SNP arrays. Furthermore, we and other groups have developed novel algorithms for detecting copy number changes at both the gene level and the allelic level (Bignell *et al.*, 2004; Zhao *et al.*, 2004; Ishikawa *et al.*, 2005; Nannya *et al.*, 2005).

In the present study, we applied a newly developed Genome Imbalance Map (GIM; Ishikawa *et al.*, 2005) algorithm to analyse genomic alterations in clinical specimens of hepatocellular carcinoma (HCC). We demonstrated the robustness of GIM analysis based on genotyping arrays in the accurate analysis of copy number alterations and allelic imbalance in the cancer genome in a single experiment. Furthermore, by integrating the gene expression data with genomic alterations, we have demonstrated that genomic alterations are reflected in the gene expression profile (Kano *et al.*, 2003; Midorikawa *et al.*, 2004). Our results confirmed a positive correlation between genome dosage and transcription.

Results

Genome Imbalance Map can detect regions of genome imbalance in hepatocellular carcinoma samples

Gene and allele copy number analyses were performed in all 36 HCC samples by taking the copy numbers of peripheral blood lymphocytes as matched controls (Figure 1). Using a 10K SNP array, the mean call rate and mean heterozygous call rate in HCC and controls were 93.4 ± 2.7 and 27.4 ± 3.2 and 95.9 ± 1.9 and $31.0 \pm 0.9\%$, respectively. The signal intensity ratio and the GIM figure in each sample from the array data are available online (http://www.genome.rcast.u-tokyo.ac.jp/GIM_HCC/).

Gains on chromosome arms of HCC were observed on 1q (72.2%), 5p (25.0%), 5q (30.5%), 6p (33.3%), 7q (22.2%), 8q (61.1%), 17q (25.0%) and 20q (25.0%), and LOH was detected on 1p (22.2%), 4q (27.7%), 6q (27.7%), 8p (55.5%), 10q (33.3%), 13q (47.2%), 16p (25.0%), 16q (36.1%) and 17p (66.7%) (Figure 2). Amplification was also observed on 5p15, 6p24, 7q31, 10p11, 11q14, 11q32 and 17q12 in each case, and the possible genes in these regions are summarized in Table 1.

To provide a comparison between our data and previously reported observations of LOH of HCC obtained by comprehensive allelotyping studies, chromosomal arms with LOH in HCC are summarized in Table 2. Most regions with LOH, as determined by GIM, have also been indicated in previous studies using comprehensive allelotyping, with the exception of 1q in which our data indicated chromosomal gains in 25 cases and UPT in two cases, and 9p of which the percentage of LOH was 19.4%. Most regions with chromosomal gains were also consistent with those determined by CGH, as reported previously (data not shown).

Regions of allelic imbalance in hepatocellular carcinoma

We found UPD and UPT in 13 samples, that is, uniparental remaining alleles duplicated or triplicated where LOH was demonstrated – the regions on 1p, 1q, 2p, 2q, 3p, 6q, 9p, 9q, 10q, 12p and 13q. To confirm UPD in these regions, we performed fluorescent *in situ* hybridization (FISH) and SNP-based LOH analysis on 13q arm and also showed UPT on 1q arm (Figure 3a and e).

Single-nucleotide polymorphism analysis at rs1336934 (SNP1) and rs1392000 (SNP2) demonstrated heterozygosity of SNP1 and 2 in the blood sample from patient 19. To further verify LOH in this specimen, we sequenced PCR fragments encompassing SNP1 and 2 and confirmed the LOH at these SNP loci. The LOH on 13q31.2–34 in patient 19 is shown in Figure 3b. On the other hand, FISH analysis using bacterial artificial chromosome (BAC) clones RP11-40H10 and RP11-14C20 verified disomy on 13q32.1-13qter in patient 19 (Figure 3c), indicating that this patient has UPD on 13q32.1-13qter. Similarly, UPD regions on 13q were confirmed in patients 11 and 21 (data not shown). In addition, 13q in patient 19 was composed of a monosomic region (13q14.11–13q31.1) and a UPD region (13q31.2–13q34) consecutively by GIM, which was clearly demonstrated by FISH analysis with BAC clones RP11-118K20 and RP11-14C20 (Figure 3d).

Furthermore, in patients 27 and 29, we observed LOH on 1q arm despite three copies of the remaining allele. Single-nucleotide polymorphism analysis at rs724781 (SNP3), rs1395548 (SNP4) and rs157864 (SNP5), and FISH analysis by RP11-89N3 corroborated the microarray data, that is, co-occurrence of LOH and trisomy on 1q in patient 27 (Figure 3f and g).

Through these results, allelic imbalance regions identified by GIM, UPD or UPT were validated by SNP analysis and FISH analysis.

Fractional copy number is owing to heterogeneity of cancer cells

Genome Imbalance Map analysis showed an intermediate pattern in nine cases, possibly reflecting a mixture of more than two heterozygous populations of liver cancer cells, which suggested chromosomal instability or heterogeneity of the tumor. Among 10 cases in which we examined copy number by FISH at three loci, we observed heterogeneity in two cases at different loci: 1p in one and 1q in the other. Heterogeneity of imbalanced loci is not dependent on chromosomal regions but rather seems to be specific to samples, because heterogeneity was often seen in multiple regions (five of nine cases), and was observed notably in poorly differentiated tumors (four of seven PD cases).

The estimated copy number was approximately 1.5 at 1p arm in patient 27 (Figure 3e). Fluorescent *in situ*

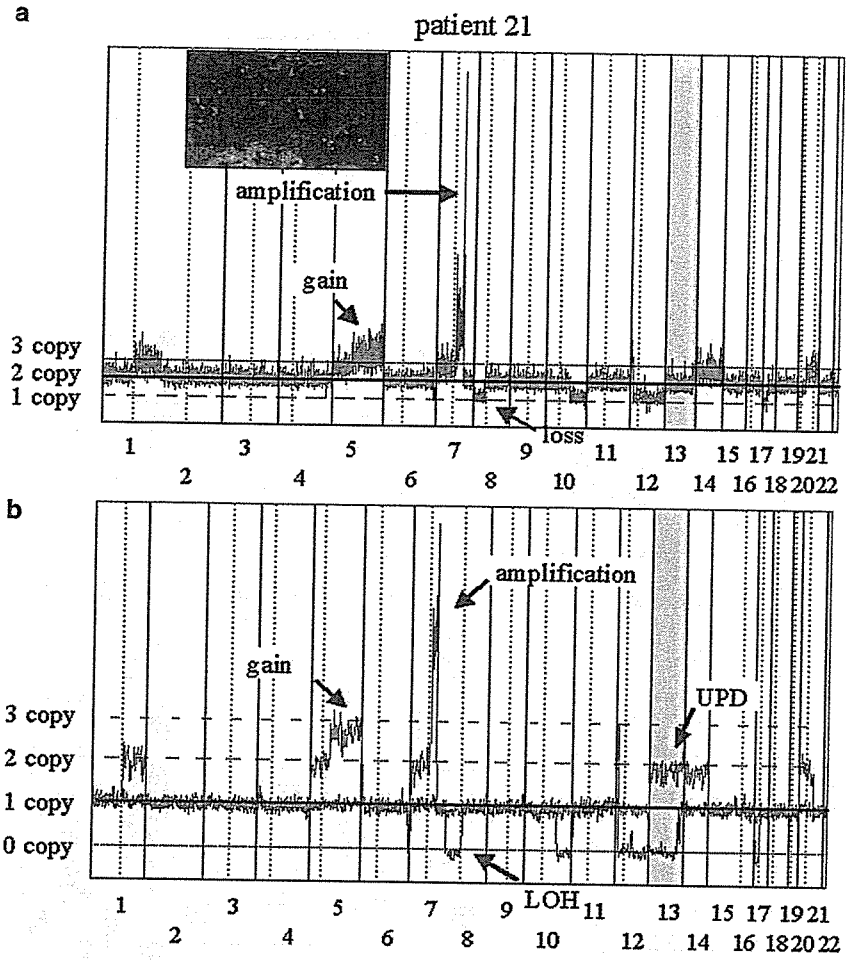

Figure 1 Genome Imbalance Map (GIM) of a representative hepatocellular carcinoma (HCC) sample. (**a**) Total gene dosage analysis across the whole genome in patient 21. Annotated copy numbers were estimated from the allelic dosage analysis as described elsewhere. Regions of copy number alteration are indicated by arrows. The inset shows amplification of *c-MET* on 7q31.2 by fluorescent *in situ* hybridization (FISH). Orange: RP11-163C9 (*c-MET*); green: CEP7. (**b**) Allelic dosage analysis across the whole genome in patient 21. Alleles with higher and lower copy numbers are connected by red and blue lines, respectively. Regions with gain, loss of heterozygosity (LOH), amplification and uniparental disomy (UPD) are indicated with arrows. Gain regions, 1q21.3-1qter, 5p, 5q, 7p, 7qcen-7q31.31, 12p13.2–12p13.3, 13q32.3-13qter, 14q, 20p, 20q; LOH regions, 6q26–6q27, 8p12.2–8p23, 10q22.2-10qter, 12pcen-12p12.3, 12q, 17p; amplified region, 7q31.2; and UPD region, 13qcen-13q32.1.

hybridization analysis showed that cancer cells are composed of those with one or two copies at nearly the same ratio, whereas chromosomes of all the corresponding hepatocytes have two copies of 1p arm (Figure 3h and i), indicating that fractional copy number in GIM reflects the heterogeneity of cancer cells.

PLAGL1 *gene as a candidate gene responsible for hepatocarcinogenesis*

A putative tumor suppressor gene, the *PLAGL1* locus on chromosome 6q24–25, was recently identified as an imprinted region (Abdollahi *et al*., 1997) and allelic loss of the long arm of chromosome 6 has also been reported in many types of human cancer (Taguchi *et al*., 1993; Thrash-Bingham *et al*., 1995). We observed LOH in eight of 36 patients, including UPD in two patients, and therefore we analysed the epigenetic status of *PLAGL1* and its expression levels.

We examined methylation status of the promoter region of the *PLAGL1* gene using methylation-specific PCR (MSP) on 15 specimens, including eight cases with LOH (two of which were UPD) and seven with retention of heterozygosity (ROH), after confirmation of the methylation status of both the background liver and lymphocytes from the patient (Supplementary Figure S1). Seven of the eight LOH (+) tumors were methylated, whereas all of the patients with ROH had both methylated and unmethylated *PLAGL1* promoter alleles (Figure 4a). In accordance with methylation status, reduction of *PLAGL1* gene expression in HCC was observed by quantitative PCR (qPCR) (Figure 4b). The expression ratio in patient 19, who has allelic loss of 6q arm and unmethylated promoter region in *PLAGL1*, was similar to those in patients with ROH of 6q. These observations suggested that the imprinted gene, *PLAGL1*, is often silenced by allelic loss and could be a candidate gene involved in hepatocarcinogenesis.

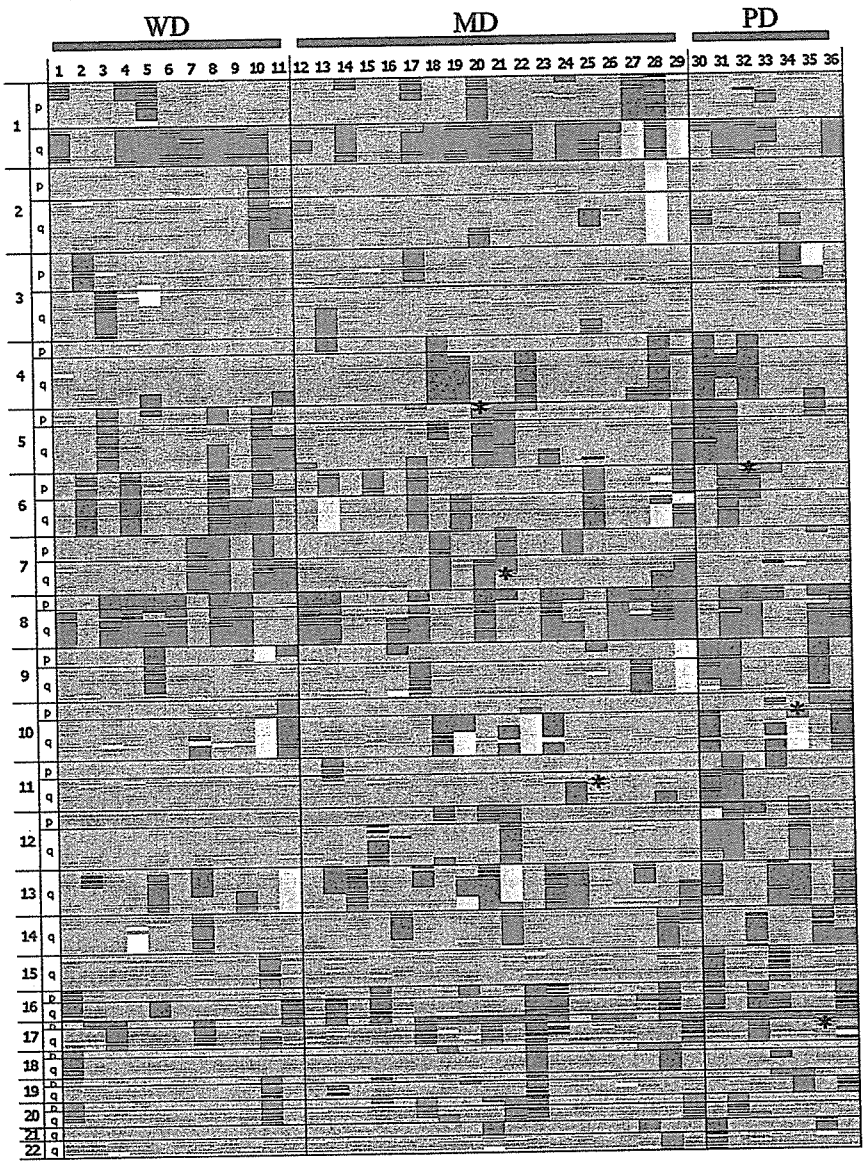

Figure 2 Overview of genome imbalance. Patient number and chromosome sites are indicated horizontally and vertically, respectively. Chromosome alteration groups: red, gain; green with asterisk, amplification; blue, LOH; yellow, uniparental disomy (UPD); gray, retention; white, not informative. WD, MD and PD indicate well, moderately and poorly differentiated hepatocellular carcinoma (HCC), respectively.

Table 1 Candidate genes in amplified regions

Amplified regions	*Candidate genes*	*Patient no.*
5p15.31	*ADCY2, MGC5297, MTRR*	20
6p24.3	*RREB1, SSR1, CTAG3, RIOK1, DSP, C6orf151*	32
7q31.2, 7q31.31	*CAV2, CAV1, MET, CAPZA2, ST7, WNT2, ASZ1, CFTR, CTTNBP2, CYR61, LSM8, ANKRD7*	21
10p11.21	*PARD3, CUL2, CREM, C10orf9, CX40.1, FZD8*	34
11q14.1, 11q32.1	*MGC33846, PRCP, FLJ25416*	25
17q12	*ACACA, FLJ39647, TADA2L, DUSP14, AP1GBP1, DDX52, TCF2, LOC414059, MRPL45, SOCS7, ARHGAP23, SNIP, MLLT6, PCGF2, PSMB3, PIP5K2B, FLJ20291, RPL23, LASP1, FLJ43826, LOC284107, PLXDC1, CACNB1, RPL19, FBXL20*	35

Gene expression profiles reflect chromosomal alterations

To confirm that alterations in mRNA expression level reflect gain or loss of genomic copy number, we compared the expression intensity with the genome dosage in the same samples (Figure 5).

Based on the expression data of patient 11, the HCC/liver normalized intensity ratio was mapped on the chromosomal regions (Figure 5a). When we compared gene expression levels with gene dosage obtained by GIM analysis in the same sample, increases were

Table 2 Chromosomal arms with LOH by GIM and comprehensive allelotyping analysis in HCC

	GIM	*Jou*	*Laurent-Puig*	*Okabe*	*Kondo*	*Piao*	*Boige*	*Nagai*
1p	22.2	60.4	33		38	22.7	44	26
1q		75	22		38	68.1		24
2q		56.5			24			29
4p						22.2		
4q	27.7	83.3	38	48	54	72.7	42	40
5q		50				28.6		
6q	27.7	52	29	36.4	44	27.2	35	36
7p		60.4			21			30
8p	55.5	70.8	48	56.5	64	63.6	60	42
8q						77.3		23
9p		50	20		25	23.1	30	21
9q								20
10q	33.3	75				33.3		27
12p		52						
13q	47.2	79.1	31	32.4	36	40	29	32
14q		72.9				46.1		20
15q		45.8						
16p	25.0		24		23	23.5	40	22
16q	36.1	70.8	30	43.3	71	59.1	39	28
17p	66.7	91.6	45	54.5	54	46.2	48	33
17q		72.9						21
18q		81.2						
21q		50			33			

Abbreviations: LOH, loss of heterozygosity; GIM, Genome Imbalance Map; HCC, hepatocellular carcinoma. Figure means percentage of LOH-positive regions that were defined as more than 20%.

observed in levels of expression of genes on 5q, 6p, 7q and 10p, regions in which genomic copy number also showed an increase. On the other hand, expression levels of genes on 2q, 4q, 9p, 10q, 16q and 17p, which were demonstrated to be LOH regions in this sample, were decreased. As shown in Figure 5b, average expression level of each gene increased in accordance with genome dosage ($P<0.00001$, Student's *t*-test).

These results demonstrated that gene expression levels tend to change according to the chromosomal copy number and that gene expression profiles reflect genome alteration.

Discussion

We used GIM analysis with genotyping arrays to generate high-throughput information on not only DNA copy number changes but also allelic imbalance for HCC samples. Our results indicated that GIM can detect the allelic status more accurately than methods used previously (Kusano *et al.*, 1999; Niketeghad *et al.*, 2001). For example, several HCC samples analysed in the present study had UPD or UPT, which may be missed or recognized as gain regions by CGH, as both CGH and array-based CGH can only detect total copy changes (Hashimoto *et al.*, 2004; Katoh *et al.*, 2005; Patil *et al.*, 2005). Uniparental disomy or UPT are exceptional derivations of a pair of offspring chromosomes from one parent only (Engel, 1980) and cause an increased risk of recessive disorders, such as Wiedemann–Beckwith (Henry *et al.*, 1991), Prader–Willi (Nicholls *et al.*, 1989) and Angelman syndromes (Malcolm *et al.*, 1991) owing to reduction to homozygosity (Engel, 1993). Furthermore, UPD regions have been shown to contain genes responsible for carcinogenesis, which have been implicated in Wilms' tumor (Grundy *et al.*, 1994), leukemia (Raghavan *et al.*, 2005) and breast cancer (Murthy *et al.*, 2002), but have never been described in HCC. Our data showed that UPD is frequently observed on chromosome 6q, 10q and 13q, where LOH is observed repeatedly and contains suppressor genes, such as *PTEN*, *DMBT1*, *BRCA2*, *RB* and *DLC2*. Therefore, UPD in 6q, 10q and 13q, resulting in duplication of mutated alleles, could be a mechanism for this inactivation.

Among the altered chromosomal regions, 6q was particularly intriguing, because imprinting gene clusters have been reported in this region (Temple *et al.*, 1995). We examined whether simultaneous epigenetic changes, such as methylation, occur in these genes. The *PLAGL1* gene, which is located on chromosome 6q24–25, inhibits tumor cell growth through induction of apoptotic cell death and G1 arrest (Varrault *et al.*, 1998). *PLAGL1* has been suggested to be a tumor suppressor gene in ovarian cancer (Cvetkovic *et al.*, 2004), and has recently been demonstrated to be regulated in an epigenetic manner (Abdollahi *et al.*, 2003). In the present study, in tumors with LOH or UPD, we found methylation of CpG islands of *PLAGL1* of the remaining allele by MSP, and marked reduction of expression intensity in accordance with methylation status using qPCR in cancerous tissues. Thus, if we overlooked UPD in this region and erroneously considered it to be in ROH status, the explanation of epigenetic alteration in this case would be obscure.

Second, GIM analysis provides accurate allelotyping in clinical specimens. Previous allelotyping studies on HCC indicated LOH in 1q, 7p and 8q, in which most samples in the present study showed genomic gain without LOH (Boige *et al.*, 1997; Nagai *et al.*, 1997; Piao *et al.*, 1998; Kondo *et al.*, 2000; Okabe *et al.*, 2000; Laurent-Puig *et al.*, 2001; Jou *et al.*, 2004). This discrepancy may be owing to severe 'allelic imbalance,' based on the polyploidy often observed in HCC, despite ROH. As allelotyping studies are often based on PCR assays at microsatellite loci, bias in amplification between alleles and contamination with DNA from normal cells is possible. Therefore, marked differences in signal intensity between two alleles may be explained as LOH, resulting in misunderstanding of allelic imbalance. Genome Imbalance Map showed that seven of 36 cases (19.4%) harbored LOH in 9p, which most researchers have demonstrated as a region of LOH, and therefore the present data were consistent with those of previous studies (Table 2).

Although we identified amplification on 5p15, 6p24, 7q31, 10p11, 11q14, 11q32 and 17q12 in each case, we have not discussed homozygous deletion in this report, because the probe density on the 10K array is not sufficiently dense to allow detection of homozygous deletions, which are usually extremely small. It should be possible to detect more homozygous deletions with a higher density SNP array. Nevertheless, we observed one homozygous deletion at 8p in two cases, which has

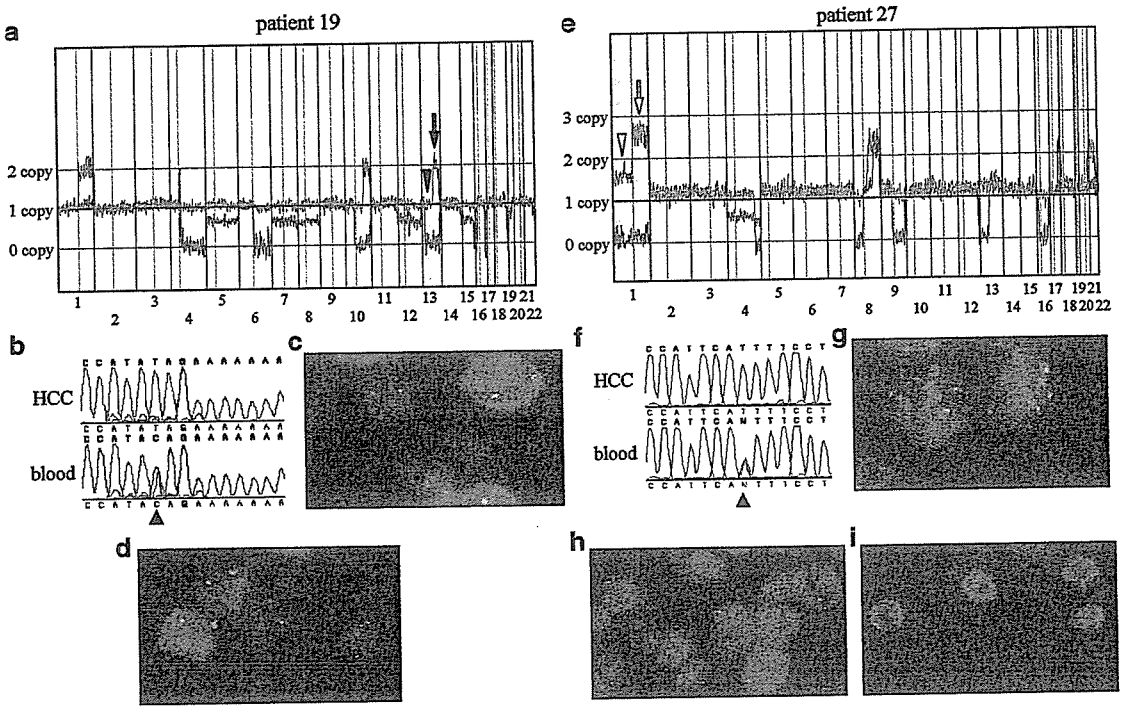

Figure 3 Fluorescence *in situ* hybridization and loss of heterozygosity (LOH) analysis for validation of allelic imbalance in 1q and 13q arms in patient 19 (**a–d**) and patient 27 (**e–h**). Genome Imbalance Map (GIM) shows LOH in 13q12.11–32.1 and uniparental disomy (UPD) in 13q31.2–34 regions in patient 19 and uniparental trisomy (UPT) in 1q arm in patient 27. (**a** and **e**) Genome Imbalance Map of patients 19 and 27, respectively. Black arrow, RP11-40H10 and RP11-14C20 (**c**); black arrowheads, RP11-118K20 (**d**); white arrow, RP11-89N3 (**g**); white arrowhead, RP11-79B11 (**h** and **i**). (**b** and **f**) Single-nucleotide polymorphism (SNP) analysis using direct sequence at rs1336934 (SNP1) (C/T) in patient 19 and at rs157864 (SNP5) (C/T) in patient 27 (arrowhead) demonstrated LOH on 13q arm and 1q arm in patients 19 and 27, respectively. (**c**) Fluorescent *in situ* hybridization (FISH) analysis demonstrated two pairs of distinct signals in liver cancer cells. Orange: RP11-40H10 (13q31.3–32.1); green: RP11-14C20 (13q32.2). (**d**) One orange signal (13q31.1) and two green signals (13q32.2) were found in liver cancer cells. These data confirmed that patient 19 had UPD in 13q31.2–34 and a breakpoint between 13q31.1 and 13q31.2. In patient 27, GIM showed UPT on 1q arm and fractional copy number on 1p arm. (**g**) Chromosome 1 centromere (orange) and 1q32.2 (green) in a frozen section of hepatocellular carcinoma (HCC). Three pairs of two distinct signals were observed in liver cancer cells. (**h** and **i**) Using FISH analysis, mixed cancer cells with one copy and two copies of 1p arm are shown (**h**). On the other hand, all the noncancerous liver cells had two signals (**i**). One signal was observed in 61.2% of all tumor nuclei, whereas the percentage of nuclei with normal copy number was only 16.2% in the control normal liver parenchyma. Orange: 1p31.3.

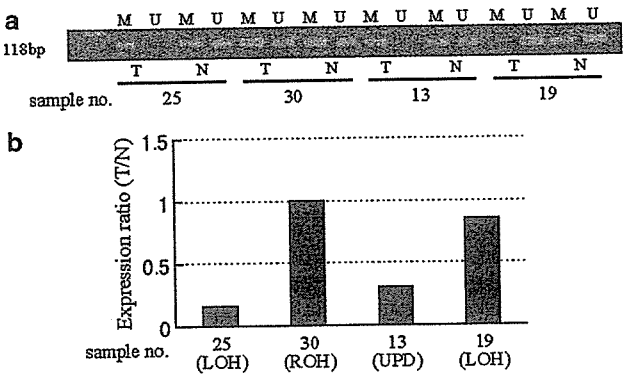

Figure 4 Epigenetic regulation of 6q24–25. (**a**) Methylation status of the promoter region of the *PLAGL1* gene by methylation-specific PCR. M, methylated; U, unmethylated; T, liver cancer; N, background liver. ΦX174 DNA-HAE III digest was used for a marker. (**b**) Analysis of *PLAGL1* gene expression in liver cancer by quantitative PCR (qPCR). Expression ratio was calculated as fold difference from the background liver.

been validated by PCR with STS markers in this region, and further analysis of these homozygous deletions is now in progress.

Furthermore, GIM often shows fractional allelic copy number, which is caused by mixture of cancer cells with different copy numbers in certain regions. Such patterns involving two levels of heterozygous deletion were previously documented using array-based CGH (Benetkiewicz *et al.*, 2005; Buckley *et al.*, 2005). In this study, we confirmed that fractional allelic copy number is owing to heterogeneity of cancer cells using FISH analysis, and is not owing to contamination by surrounding normal cells, because the GIM algorithm can be applied when the ratio of contamination of the surrounding normal cells is less than 50% (Ishikawa *et al.*, 2005) and the tumor cells occupied more than 90% in the HCC samples used in this study (Supplementary Figure S2). Fluorescent *in situ* hybridization analysis showed that one allele was lost completely in all the tumor cells, implying that the one or two copies of 1p observed in the tumor cells with two copies were copies of the remaining allele, whereas the cells with one copy did not have such copies, which may duplicate in future resulting in UPD on 1p arm in patient 27.

We and other groups reported previously that genome dosage reflects expression imbalance (Pollack *et al.*,

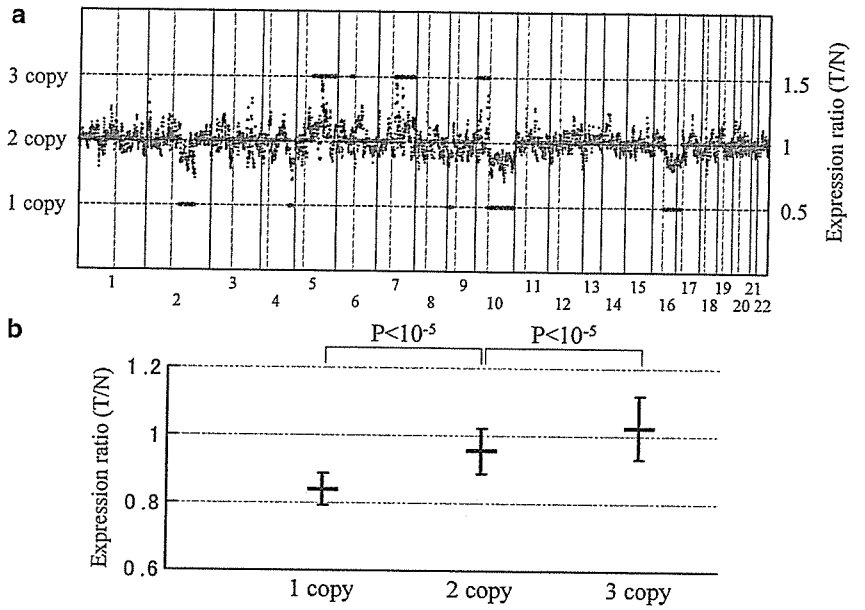

Figure 5 Comparison of genomic alteration and gene expression status. (**a**) Total gene dosage and expression analysis across the whole genome of patient 11. Blue dots represent hepatocellular carcinoma (HCC)/liver expression intensity ratio and red continuous lines indicate copy numbers. After normalization as described in Materials and methods, gene expression intensity ratio was computed within a 5 Mb moving average and plotted. In patient 11, gains were observed on 5q, 6p, 7q and 10p, and loss of heterozygosity (LOH) was observed on 2q, 4q, 9p, 10q 15q and 16p. Gene expression levels changed in accordance with genomic alterations. (**b**) Both the average and standard deviation of expression intensity ratio were calculated for each copy number. Differences at $P<0.01$ were considered statistically significant.

2002; Midorikawa *et al.*, 2004). Upender *et al.* (2004) demonstrated that genomic aneuploidy affects gene expression pattern using the chromosome transfer model. To confirm these observations, the effects of genome imbalance on the transcriptome were validated by direct comparison with expression data from the same samples in the present study. Previously, we also demonstrated stepwise chromosomal expression changes in the progression of HCC (Midorikawa *et al.*, 2004), that is, expression gain in 1q and 8p, and loss of 8p, 13q and 17p were observed in well-differentiated liver cancer, whereas expression gains in 12q, 17q and 20q, and reduction in 4q were demonstrated only in advanced HCC. On the other hand, GIM showed frequent allelic gains at 1q, 5q, 6p and 8q, and LOH at 8p and 16q regardless of cancer differentiation grade, and gains at 12q and LOH at 15q were detected specifically in poorly differentiated tumors. In nine positive chromosomal regions identified in the Expression Imbalance Map (EIM), the present data observed by GIM were consistent with our previous observations, that is, poorly differentiated grade tumors contained more chromosomal aberrations in these regions (Supplementary Figure S3). However, gains at 5p, 5q, 6p and 7q, and LOH at 1p, 6q, 16p and 16q, which were detected by GIM, were not identified using EIM, partly because we determined the positive region based on the range of alteration (>3 Mb), which is affected by the density of probes. We used a U95A expression array (Affymetrix, Santa Clara, CA, USA), which includes about only 12 000 probes in EIM analysis in our previous study, and availability of much higher-density arrays will make it possible to identify more altered regions, such as gain at 5p, 5q, 6p and 7q, and LOH at 1p, 6q, 16p and 16q, using EIM.

We applied genotyping array analysis to study genome imbalance in liver cancer using a recently developed method for signal standardization. Comparison of our observations with those of previous studies on chromosomal imbalance by CGH and comprehensive allelotyping localizes the particular chromosomal alterations that conventional methods may overlook or miscomprehend their importance validated by FISH and LOH analysis. This method has the advantage that genome dosage and allelic imbalance, including cancer-specific genomic alterations, can be observed simultaneously, which could lead to the identification of responsible genes with both ease and a high degree of reliability.

Materials and methods

Patients and tissue samples

In all, 36 patients with HCC undergoing hepatectomy in the Hepato-Biliary-Pancreatic Surgery Division, Department of Surgery, Graduate School of Medicine, University of Tokyo were recruited in this study. All subjects gave their informed consent to participation in the study. Among the 36 patients with HCC, 14 were positive for hepatitis B surface antigen (HB), 19 for hepatitis C viral antibody (HC), one for both HB and HC and two for neither HB nor HC. High-density genotyping microarrays (GeneChips) from Affymetrix were used for analysis of primary tumor and peripheral blood samples. Clinical parameters and tumor status based on

histological findings of resected specimens are summarized in Supplementary Table S1.

The surgical specimens were immediately cut into small pieces after resection, snap frozen in liquid nitrogen and stored at −80°C.

Genomic DNA extraction and oligonucleotide microarray

Genomic DNA was isolated from tumor tissues or lymphocyte pellets using a QIAamp DNA Mini Kit (Qiagen, Valencia, CA, USA), according to the manufacturer's specifications. Experimental procedures for GeneChip™ were performed according to GeneChip Expression Analysis Technical Manual (Affymetrix, Santa Clara, CA, USA), using a Human Mapping 10K Array *Xba*I 131 kit (Affymetrix).

Genome Imbalance Map

The GIM algorithm was applied to raw data of HCC and peripheral blood obtained from SNP arrays. Gene locus information was obtained from the websites for Genes On Sequence Map (*Homo sapiens* build 34). The basic concept of GIM involves normalization of probe-level signals, as described previously (Ishikawa *et al*., 2005). Briefly, the signal intensity ratio between the raw signal intensity from the cancer and paired normal samples was calculated from the perfect match (PM) probes for each SNP locus by taking the median after omitting the highest and lowest values. Second, we calculated the adjusted ratio, which is the raw ratio divided by the expected ratio. The expected ratio is calculated by adjusting several parameters for each experiment, for example, length of *Xba*I fragment, percentage of GC of *Xba*I fragment, local GC content, hybridization free energy of 25-mer probe sequences and genomic mean of signal intensity of PM probes from reference sample.

Fluorescent in situ *hybridization and single-nucleotide polymorphism-based loss of heterozygosity analysis*

Fluorescent *in situ* hybridization analysis, and LOH analysis at SNP loci (SNP analysis) were performed to validate the interpretation of the GIM analysis. We obtained nine genomic BACs from a human BAC library (Advanced Geno Techs Co., Tsukuba, Japan), which contained the following regions: RP11-79B11 for 1p31.3 (used for FISH analysis of patient 27), RP11-89N3 for 1q32.2 (patients 27 and 29); RP11-90B18 for 10q23.3 and RP11-166J24 for 10q23.31 (patients 10, 19 and 22); and RP11-93G2 for 13q31.1, RP11-118K20 for 13q31.1, RP11-40H10 for 13q31.3-32.1 and RP11-14C20 for 13q32.2 (patients 11, 19 and 21). The relationships of the BAC clones to the SNP probes are summarized in Table 3 and Supplementary Figure S4. Sections (5 μm thick) were cut from fresh–frozen liver cancer and background liver tissues, which were fixed in 80% ethanol for 24 h, embedded in paraffin and arranged in a tissue microarray, and were used for microwave-assisted FISH analysis (Kitayama *et al*., 2003). Bacterial artificial chromosomes clones were labeled with Alexa 546 and 488 (Molecular Probes, Eugene, OR, USA) by nick translation. With regard to centromere enumeration probes, Spectrum Green-labeled CEP10 and Spectrum Orange-labeled CEP1 (Vysis Inc., Downers Grove, IL, USA) were used with differently labeled RP11-79B11 and RP11-89N3; RP11-90B18 and RP11-166J24, respectively. Hybridization and evaluation of the results were performed as described previously with minor modifications (Kitayama *et al*., 2003). DAPI I (4,6-diamidino-2-phenylindol, 1000 ng/ml; Vysis Inc.) was used for nuclear counterstaining. The samples were promptly observed using a fluorescence microscope (BX-51; Olympus, Japan, Tokyo, Japan) equipped with epifluorescence filters and a photometric CCD camera (Sensicam; PCO Company, Kelheim, Germany). The number of FISH signals per cell was counted for a total of more than 100 intact and non-overlapping cell nuclei. Furthermore, to prevent counting of 'artificial loss' by missing the part of the nuclei in tangential views, we applied the same method in the background liver and the cutoff value for background was intentionally set at a higher percentage, up to 20% (Sano *et al*., 2006).

Table 3 Relationship of BAC clones and SNP probes used in FISH analysis

BAC clone	*SNP probe*	*Chromosomal loci*	*Patient no.*
RP11-79B11	rs1390474, rs596504, rs556670	1p31.3	27, 29
RP11-89N3	rs616544, rs724054, rs2357212, rs1340128	1q32.2	27, 29
RP11-90B18	rs4623300, rs956422	10q23.3	10, 19, 22
RP11-166J24	rs1936614, rs2254391	10q23.31	10, 19, 22
RP11-93G2	rs1986644, rs1931046	13q31.1	11, 19, 21
RP11-118K20	rs4129856, rs1541071	13q31.1	11, 19, 21
RP11-40H10	rs1927493, rs2009772	13q31.3-32.1	11, 19, 21
RP11-14C20	rs966458, rs2892734	13q32.2	11, 19, 21

BAC, bacterial artificial chromosome; FISH, fluorescent *in situ* hybridization; SNP, single-nucleotide polymorphism. SNP probes are described based on refSNP ID number of dbSNP database (http://www.ncbi.nlm.nih.gov/projects/SNP).

Single-nucleotide polymorphism analysis was applied to assess LOH in UPD regions determined by GIM. A search was performed for SNPs on 1q and 13q arms in the National Center for Biotechnology Information's SNP database. SNPs within 500 bp were amplified by PCR using the following flanking primers and genotyped by direct sequencing:

SNP1 Forward primer 5′-GATTGGTTCCAGGACTAGAG-3′
Reverse primer 5′-GAAAGTGCCAAGCTGTACAC-3′
SNP2 Forward primer 5′-TTCACTCACTCTGGGCTATC-3′
Reverse primer 5′-TCAACAGCTCCCCTTGATAC-3′
SNP3 Forward primer 5′-CCTACTTTTCCTCCCCTTTG-3′
Reverse primer 5′-CCATGCTGGGATCTTGAATG-3′
SNP4 Forward primer 5′-AGCTAAGAGCCAACTCTAGC-3′
Reverse primer 5′-CACTCTTTCTCCTCTTGCTC-3′
SNP5 Forward primer 5′-AACGAACCACAGTTCCCAAC-3′
Reverse primer 5′-TGGATACTCCTTGGAGCTTC-3′

Disappearance of heterozygosity on informative SNPs in tumors was considered to be LOH.

Bisulfite modification and methylation-specific polymerase chain reaction and quantitative polymerase chain reaction

Aliquots of 2 μg of genomic DNA extracted from cancerous tissues and from the background liver and lymphocytes of the same patients as controls were treated with sodium bisulfite (Sigma, St Louis, MO, USA) and used for MSP, as described previously (Herman *et al*., 1996). Bisulfite-modified DNA was amplified with *PLAGL1* gene-specific primers:

M-S 5′-TTGTTTAAACGTGAGTATTGATCGT-3′
M-AS 5′-TTCGTTTCTTCAACTATAA AACGAA-3′
UM-S 5′-TTGTTTAAATGTGAGTATTGATTGT-3′
UM-AS 5′-CTTCATTTCTTCAACTATAAAACAAA-3′

The PCR conditions consisted of denaturation of template at 94°C for 15 min and successive cycles of 94°C for 30 s, 60°C for methylation-specific or 58°C for unmethylated primers for

1 min, and 72°C for 1 min, with a final extension 72°C for 5 min. Reaction products were separated by electrophoresis on 2% agarose gels, stained with ethidium bromide and photographed.

Quantitative polymerase chain reaction for detecting expression of *PLAGL1* gene was performed using an iCycler (Bio-Rad, Hercules, CA, USA). The primers and PCR conditions used were as described previously (Cvetkovic *et al.*, 2004). After relative quantification by measuring the ratio between the mean value of the target gene and that of β-actin in each sample, *PLAGL1* mRNA expression was compared with the background liver.

RNA extraction and oligonucleotide microarray for gene expression studies

Total RNA was isolated from HCC and the background liver as described previously (Midorikawa *et al.*, 2002). Experimental procedures for CodeLink Human Whole Genome Bioarray were performed according to the manufacturer's specifications (Amersham Biosciences, Piscataway, NJ, USA), using 10 μg of total RNA.

Normalization and filtering of intensity of gene expression

Before further statistical analysis, we normalized and filtered the raw data. A quantile normalization procedure was used for the probe intensity distribution across different chips. The average of expression level intensity, the normalized intensity, was scaled to 1, and each expression data sets where the normalized intensity values were less than 1 were excluded from analysis.

Comparison of gene expression with gene dosage

To parallelize gene dosage and gene expression data, we average both gene copy number by SNP array analysis and expression ratio (HCC/liver) by expression microarray analysis in 100-kb windows. The 100-kb averaged value was smoothed within a 5-Mb moving median. Low probe density regions (less than 1 probe in 5 Mb window) were eliminated from analysis.

Acknowledgements

We thank Hiroko Meguro, Kunihiro Nishimura, Akira Watanabe, Kimihiro Yamashita, Megumi Ihara and Kiyoko Nagura for valuable technical assistance, and Panda Binaya for helpful discussion. This work was supported in part by a Grant-in-Aid for Scientific Research (S) 16101006 (HA) and (C) 17591378 (YM), Scientific Research on Priority Areas 17015008 (HA) and 17015017 (HS), and Special Coordination Fund for Science and Technology from The Ministry of Education, Science, Sports and Culture, and CREST, JST (HA), Mitsui Life Social Welfare Foundation (YM), Smoking Research Foundation (HS), the Program of Fundamental Studies in Health Sciences of the National Institute of Biomedical Innovation (NIBIO) and Focus 21 Project of New Energy and Industrial Technology Development Organization (NEDO).

References

Abdollahi A, Godwin AK, Miller PD, Getts LA, Schultz DC, Taguchi T *et al.* (1997). *Cancer Res* **57**: 2029–2034.
Abdollahi A, Pisarcik D, Roberts D, Weinstein J, Cairns P, Hamilton TC. (2003). *J Biol Chem* **278**: 6041–6049.
Benetkiewicz M, Wang Y, Schaner M, Wang P, Mantripragada KK, Buckley PG *et al.* (2005). *Genes Chromosomes Cancer* **42**: 228–237.
Bignell GR, Huang J, Greshock J, Watt S, Butler A, West S *et al.* (2004). *Genome Res* **14**: 287–295.
Boige V, Laurent-Puig P, Fouchet P, Flejou JF, Monges G, Bedossa P *et al.* (1997). *Cancer Res* **57**: 1986–1990.
Buckley PG, Jarbo C, Menzel U, Mathiesen T, Scott C, Gregory SG *et al.* (2005). *Cancer Res* **65**: 2653–2661.
Cvetkovic D, Pisarcik D, Lee C, Hamilton TC, Abdollahi A. (2004). *Gynecol Oncol* **95**: 449–455.
Engel E. (1980). *Am J Med Genet* **6**: 137–143.
Engel E. (1993). *Am J Med Genet* **46**: 670–674.
Grundy P, Wilson B, Telzerow P, Zhou W, Paterson MC. (1994). *Am J Hum Genet* **54**: 282–289.
Hashimoto K, Mori N, Tamesa T, Okada T, Kawauchi S, Oga A *et al.* (2004). *Mod Pathol* **17**: 617–622.
Henry I, Bonaiti-Pellie C, Chehensse V, Beldjord C, Schwartz C, Utermann G *et al.* (1991). *Nature* **351**: 665–667.
Herman JG, Graff JR, Myohanen S, Nelkin BD, Baylin SB. (1996). *Proc Natl Acad Sci USA* **93**: 9821–9826.
Hoque MO, Lee CC, Cairns P, Schoenberg M, Sidransky D. (2003). *Cancer Res* **63**: 2216–2222.
Ishikawa S, Komura D, Tsuji S, Nishimura K, Yamamoto S, Panda B *et al.* (2005). *Biochem Biophys Res Commun* **333**: 1309–1314.
Janne PA, Li C, Zhao X, Girard L, Chen TH, Minna J *et al.* (2004). *Oncogene* **23**: 2716–2726.
Jou YS, Lee CS, Chang YH, Hsiao CF, Chen CF, Chao CC *et al.* (2004). *Cancer Res* **64**: 3030–3036.
Kallioniemi A, Kallioniemi OP, Sudar D, Rutovitz D, Gray JW, Waldman F *et al.* (1992). *Science* **258**: 818–821.
Kano M, Nishimura K, Ishikawa S, Tsutsumi S, Hirota K, Hirose M *et al.* (2003). *Physiol Genomics* **13**: 31–46.
Katoh H, Shibata T, Kokubu A, Ojima H, Loukopoulos P, Kanai Y *et al.* (2005). *J Hepatol* **43**: 863–874.
Kennedy GC, Matsuzaki H, Dong S, Liu WM, Huang J, Liu G *et al.* (2003). *Nat Biotechnol* **21**: 1233–1237.
Kitayama Y, Igarashi H, Watanabe F, Maruyama Y, Kanamori M, Sugimura H. (2003). *Lab Invest* **83**: 1311–1320.
Kondo Y, Kanai Y, Sakamoto M, Mizokami M, Ueda R, Hirohashi S. (2000). *Hepatology* **32**: 970–979.
Kusano N, Shiraishi K, Kubo K, Oga A, Okita K, Sasaki K. (1999). *Hepatology* **29**: 1858–1862.
Laurent-Puig P, Legoix P, Bluteau O, Belghiti J, Franco D, Binot F *et al.* (2001). *Gastroenterology* **120**: 1763–1773.
Lieberfarb ME, Lin M, Lechpammer M, Li C, Tanenbaum DM, Febbo PG *et al.* (2003). *Cancer Res* **63**: 4781–4785.
Lindblad-Toh K, Tanenbaum DM, Daly MJ, Winchester E, Lui WO, Villapakkam A *et al.* (2000). *Nat Biotechnol* **18**: 1001–1005.
Lucito R, Healy J, Alexander J, Reiner A, Esposito D, Chi M *et al.* (2003). *Genome Res* **13**: 2291–2305.
Malcolm S, Clayton-Smith J, Nichols M, Robb S, Webb T, Armour JA *et al.* (1991). *Lancet* **337**: 694–697.
Mei R, Galipeau PC, Prass C, Berno A, Ghandour G, Patil N *et al.* (2000). *Genome Res* **10**: 1126–1137.
Midorikawa Y, Tsutsumi S, Nishimura K, Kamimura N, Kano M, Sakamoto H *et al.* (2004). *Cancer Res* **64**: 7263–7270.

Midorikawa Y, Tsutsumi S, Taniguchi H, Ishii M, Kobune Y, Kodama T *et al.* (2002). *Jpn J Cancer Res* **93**: 636–643.
Murthy SK, DiFrancesco LM, Ogilvie RT, Demetrick DJ. (2002). *Mod Pathol* **15**: 1241–1250.
Nagai H, Pineau P, Tiollais P, Buendia MA, Dejean A. (1997). *Oncogene* **14**: 2927–2933.
Nannya Y, Sanada M, Nakazaki K, Hosoya N, Wang L, Hangaishi A *et al.* (2005). *Cancer Res* **65**: 6071–6079.
Nicholls RD, Knoll JH, Butler MG, Karam S, Lalande M. (1989). *Nature* **342**: 281–285.
Niketeghad F, Decker HJ, Caselmann WH, Lund P, Geissler F, Dienes HP *et al.* (2001). *Br J Cancer* **85**: 697–704.
Okabe H, Ikai I, Matsuo K, Satoh S, Momoi H, Kamikawa T *et al.* (2000). *Hepatology* **31**: 1073–1079.
Patil MA, Gutgemann I, Zhang J, Ho C, Cheung ST, Ginzinger D *et al.* (2005). *Carcinogenesis* **26**: 2050–2057.
Piao Z, Park C, Park JH, Kim H. (1998). *Int J Cancer* **75**: 29–33.
Pinkel D, Segraves R, Sudar D, Clark S, Poole I, Kowbel D *et al.* (1998). *Nat Genet* **20**: 207–211.
Pollack JR, Perou CM, Alizadeh AA, Eisen MB, Pergamenschikov A, Williams CF *et al.* (1999). *Nat Genet* **23**: 41–46.
Pollack JR, Sorlie T, Perou CM, Rees CA, Jeffrey SS, Lonning PE *et al.* (2002). *Proc Natl Acad Sci USA* **99**: 12963–12968.
Raghavan M, Lillington DM, Skoulakis S, Debernardi S, Chaplin T, Foot NJ *et al.* (2005). *Cancer Res* **65**: 375–378.
Sano T, Kityama Y, Igarashi H, Suzuki M, Tanioka F, Chida K *et al.* (2006). *Pathol Int* **56**: 117–125.
Taguchi T, Jhanwar SC, Siegfried JM, Keller SM, Testa JR. (1993). *Cancer Res* **53**: 4349–4355.
Temple IK, James RS, Crolla JA, Sitch FL, Jacobs P, Howell WM *et al.* (1995). *Nat Genet* **9**: 110–112.
Thrash-Bingham CA, Salazar H, Freed JJ, Greenberg RE, Tartof KD. (1995). *Cancer Res* **55**: 6189–6195.
Upender MB, Habermann JK, McShane LM, Korn EL, Barrett JC, Difilippantonio MJ *et al.* (2004). *Cancer Res* **64**: 6941–6949.
Varrault A, Ciani E, Apiou F, Bilanges B, Hoffmann A, Pantaloni C *et al.* (1998). *Proc Natl Acad Sci USA* **95**: 8835–8840.
Wang DG, Fan JB, Siao CJ, Berno A, Young P, Sapolsky R *et al.* (1998). *Science* **280**: 1077–1082.
Weissenbach J, Gyapay G, Dib C, Vignal A, Morissette J, Millasseau P *et al.* (1992). *Nature* **359**: 794–801.
Zhao X, Li C, Paez JG, Chin K, Janne PA, Chen TH *et al.* (2004). *Cancer Res* **64**: 3060–3071.

Supplementary Information accompanies the paper on the Oncogene website (http://www.nature.com/onc).

Influences of Chymase and Angiotensin I-Converting Enzyme Gene Polymorphisms on Gastric Cancer Risks in Japan

Mitsushige Sugimoto,[1] Takahisa Furuta,[2] Naohito Shirai,[3] Mutsuhiro Ikuma,[1] Haruhiko Sugimura,[4] and Akira Hishida[1]

[1]First Department of Medicine, [2]Center for Clinical Research, [3]Department of Laboratory Medicine, and [4]First Department of Pathology, Hamamatsu University School of Medicine, Shizuoka, Japan

Abstract

Backgrounds and Aims: **The renin-angiotensin system plays an important role in homeostasis. Angiotensin II, which is generated by chymase and angiotensin I-converting enzyme (ACE), controls blood pressure as well as angiogenesis and cell proliferation. The aim of this study was to clarify the association of the chymase gene (*CMA/B*) and *ACE* polymorphisms with susceptibility to gastric cancer and peptic ulcer.**

Methods: **We assessed *CMA/B* A/G and *ACE* insertion/deletion (I/D) polymorphisms in *H. pylori*-positive gastric cancers ($n = 119$), gastric ulcers ($n = 127$), and duodenal ulcers ($n = 105$), and controls ($n = 294$) consisting of *H. pylori*-positive gastritis alone ($n = 162$) and *H. pylori*-negative subjects ($n = 132$) by PCR methods.**

Results: **In *CMA/B* polymorphism, the age- and sex-adjusted odds ratios (OR) of A/A and A/G genotypes relative to the G/G genotype for gastric cancer risk were 7.115 (95% confidence interval, 1.818-27.845) and 1.956 (95% confidence interval, 1.137-3.366), respectively. There was an increased risk for gastric ulcer in the A/A genotype (OR, 3.450; 1.086-10.960). However, there was no association between *ACE* polymorphism and susceptibility to gastric cancer and peptic ulcer. In allele combination analysis of *CMA/B* and *ACE* polymorphisms, the A/I allele combinations (*CMA/B* G/A or A/A and *ACE* I/I genotype) significantly increased the risk of gastric cancer development (OR, 4.749, 2.050-11.001) compared with the G/I allele combinations (*CMA/B* G/G and *ACE* I/I genotype).**

Conclusions: **The *CMA/B* polymorphism was associated with an increased risk for gastric cancer and gastric ulcer development. The genotyping test of the renin-angiotensin system could be useful for the screening of individuals with higher risks of gastric cancer and gastric ulcer.** (Cancer Epidemiol Biomarkers Prev 2006;15(10):1929–34)

Introduction

Gastric cancer remains the world's second most common malignancy (1). In 1994, the WHO/IARC designated *Helicobacter pylori* as a definite biological group 1 carcinogen of gastric cancer. For the prevention of gastric cancer and peptic ulcer diseases, eradication of *H. pylori* is recommended as the first-line therapy for patients with *H. pylori* infection (2, 3). However, so many people are infected with *H. pylori*, that it is difficult to let all *H. pylori*-infected individuals undergo the eradication therapy, and therefore, a useful tool for the selection of subjects at higher indication of eradication of *H. pylori* is desirable.

The pathogenesis and progression of gastric cancer development consists of a variety of processes, which include cell proliferation, cell differentiation, angiogenesis, and degradation of the extracellular matrix. Recently, the association of the host genetics with such processes (e.g., inflammation-related cytokine polymorphisms, cytochrome P450 enzyme polymorphisms, glutathione *S*-transferase, *N*-acetyltransferase, matrix metalloproteinase, p53, and k-ras mutation) has been intensively investigated in relation to chronic *H. pylori* infection (4-9).

The renin-angiotensin (RA) system consisting of renin, angiotensinogen, angiotensin I, angiotensin II, angiotensin I-converting enzyme (ACE), and chymase plays a key role in blood pressure regulation. A local RA system is also observed in various organs and angiotensin II is locally produced in each organ. Recently, there has been increasing evidence that angiotensin II is involved in the regulation of cell proliferation, angiogenesis, inflammation, and tissue remodeling via the angiotensin II type 1 receptors (AT1R; refs. 10-13). Therefore, the angiotensin II/AT1R pathway might be related to cancer biology.

ACE inhibitors inhibit the ACE-mediated conversion of angiotensin II from angiotensin I. A recent epidemiologic study has shown that ACE inhibitors and AT1R antagonists have inhibitory effects on tumor progression, vascularization, and metastasis, and that the stimulation of angiotensin II type 2 receptors inhibits the development of cancer (14). Therefore, the RA system has recently been focused on as the candidate target of chemopreventive therapy.

ACE in the chromosome 17q23 has six polymorphisms [e.g., *ACE*-240 A/T and the presence (insertion; I allele)/absence (deletion; D allele) of 287 bp DNA fragment in intron 16; refs. (15, 16)]. Plasma ACE levels are highest in subjects with the *ACE* D/D genotype, those with the I/D genotype come next and those with the I/I genotype are lowest of the three genotype groups (15, 16). The *ACE*-240 A allele is also associated with lower plasma ACE levels compared with *ACE*-240 T allele (17). The plasma ACE level is a critical factor in the determination of the plasma angiotensin II level, and therefore, the *ACE* I/D polymorphism has been shown to influence the risk of hypertension and other cardiac diseases (18). Recently, it has been reported that women with the low-activity *ACE* genotype are at a lower risk of the development

Received 4/26/06; revised 7/3/06; accepted 8/10/06.

Grant support: Grant-in-Aid from the YOKOYAMA Foundation for Clinical Pharmacology, from the Ministry of Health, Labor, and Welfare for the Second- and Third-Term Comprehensive 10-Year Strategy for Cancer Control (15-22), from the Smoking Research Foundation, and from the Ministry of Education, Culture, Sports, Science and Technology of Japan for Scientific Research (15290125) on Priority Area (17015017, 17590470, and 18014009) and the 21st century COE program Medical Photonics (Hamamatsu University School of Medicine), and by a Grant-in-Aid from the Foundation for Promotion of Cancer Research (H. Sugimura).

The costs of publication of this article were defrayed in part by the payment of page charges. This article must therefore be hereby marked advertisement in accordance with 18 U.S.C. Section 1734 solely to indicate this fact.

Requests for reprints: Mitsushige Sugimoto, First Department of Medicine, Hamamatsu University School of Medicine, 1-20-1 Handayama, Hamamatsu 431-3192, Japan. Phone: 81-53-435-2261; Fax: 81-53-434-9447. E-mail: mitsu@hama-med.ac.jp

doi:10.1158/1055-9965.EPI-06-0339

of breast cancer compared to those with the high producer allele/genotype (19, 20). However, the relationships between the *ACE* I/D polymorphism and the risk of gastric cancer have not fully been elucidated (21-23).

Chymase, which is a chymotrypsin-like serine protease produced in the secretary granules of mast cells, also mainly mediates the local, not systemic, generation of angiotensin II (24). There are two polymorphisms in the chymase gene (*CMA*), *CMA/A* and *CMA/B*, localized in the chromosome 14 (25). Those two polymorphisms have been shown to correlate with activity/expression of chymase, and therefore, the *CMA* polymorphism is a potential candidate for the susceptibility to hypertension, cardiovascular diseases and neoplastic diseases (25, 26).

Although the polymorphic effects of *ACE* on the development of gastric cancer have been reported (21-23), the relationships among *ACE* and *CMA/B* polymorphisms, histologic types of gastric cancer, and clinical stage are unclear. Moreover, there is no report about the association with the RA system–related gene polymorphism and peptic ulcer development. To further determine the possible role of the RA system in the development of gastric cancer and peptic ulcer in humans, we examined whether genetic polymorphisms in *CMA/B* A/G and *ACE* I/D were associated with gastric cancer and peptic ulcer risks in Japanese patients with *H. pylori* infection.

Materials and Methods

Subjects. A total of 645 Japanese patients who agreed to participate in the present study underwent gastroduodenoscopy at the University Hospital of Hamamatsu University School of Medicine from January 2001 to December 2005. Of 645 subjects, 513 patients with *H. pylori* infection on the basis of serologic testing (HM-CAP kit, Enteric Product Inc., Stony Brook, NY), rapid urease test (Helico Check, Otsuka Co., Tokushima, Japan), and/or culture, and 132 subjects without *H. pylori* infection using the above three tests, were enrolled in this study. The 513 *H. pylori*-positive subjects consisted of the gastric cancer (n = 119), gastric ulcer (n = 127), duodenal ulcer (n = 105), and gastritis alone groups (n = 162; Table 1). Each diagnosis was proven histopathologically and endoscopically. The gastric cancer group was further pathologically classified into the two subgroups, the intestinal type group and the diffuse type group, according to the Lauren classification (Table 1; ref. 27).

The protocol was approved in advance by the Human Institutional Review Board of Hamamatsu University School of Medicine. Written informed consent was obtained from each subject.

Genotyping of *CMA/B* and *ACE*. DNA was extracted from the leukocytes of each subject, using a commercially available kit (IsoQuick, ORCA Research, Inc., Bothell, WA). The *CMA/B* A/G polymorphism was determined as described by Pfeufer et al. (25). Amplification primers for the 285-bp fragment were 5′-GGA AAT GTG AGC AGA TAG TGC AGT C-3′ and 5′-AAT CCG GAG CTG GAG AAC TCT TGT C-3′. Dénaturation was done for 10 minutes at 94°C, 40 cycles of 94°C for 1 minute, 70°C for 1 minute, 72°C for 1 minute, and finally at 72°C for 7 minutes. The PCR products were digested with *Bst*XI (Takara Bio, Inc., Shiga, Japan) at 45°C for 1 hour. The genotypes were designated as follows: A/A, a single 285-bp band; A/G, three bands of 90, 195, and 285 bp; and G/G, two bands of 90 and 195 bp.

The *ACE* I/D polymorphism was identified on the basis of PCR amplification of the respective fragments from intron 16 of *ACE*, as previously reported (28). Primer sequences to determine *ACE* I/D polymorphism by PCR method are 5′-GCC CTG CAG GTG TCT GCA GCA TGT-3′ and 5′-GGA TGG CTC TCC CCG CCT TGT CTC-3′. The PCR conditions were run at 94°C for 10 minutes, then 35 cycles of 94°C for 1 minute, 70°C for 1 minute, 72°C for 1 minute, and finally at 72°C for 7 minutes. The genotypes were designated as follows: I/I, a single band of 597 bp; D/I, two bands of 319 and 597 bp; and D/D, a single band of 319 bp (28). Because the D allele in heterozygous subjects is preferentially amplified, there is a tendency for misclassification of the *ACE* I/D genotype as the D/D genotype (4-5%; ref. 28). In order to avoid this misclassification, a second independent PCR was done with a primer pair that recognizes insertion-specific sequences (5′-TGG GAC CAC AGC GCC CGC CAC TAC-3′ and 5′-TCG CCA GCC CTC CCA TGC CCA TAA-3′), with identical PCR conditions. The reaction yields a 335 bp amplicon only in the presence of an I allele, and no product in *ACE* D/D genotype.

Assay of Serum Pepsinogen Levels. Gastric atrophy and inflammation are an important abnormality associated with the development of gastric ulcer and gastric cancer. Although histologic examination of the gastric mucosa is the most accurate method of assessing gastric atrophy and inflammation, it is possible to use a functional surrogate marker for this purpose. Severe corpus inflammation and atrophy are associated with a reduction in the pepsinogen (PG) I level and the PG I/PG II ratio, and both have been used as surrogate markers of gastric atrophy and inflammation (29, 30). Then, we measured serum levels of PG I and PG II levels by RIA (Abotto Japan, Tokyo, Japan), and the PG I/PG II ratio was calculated for the serologic assessment of gastric atrophy in >50-year-old patients with *H. pylori* infection.

Table 1. Demographic characteristics and frequencies of *CMA/B* A/G and *CEA* I/D polymorphisms

	H. pylori-negative (n = 132)	Gastritis alone (n = 160)	Gastric ulcer (n = 127)	Duodenal ulcer (n = 105)	Gastric cancer (n = 119)	P
Age, y (mean ± SD)	53.8 ± 1.0	51.4 ± 0.9	52.3 ± 1.1	50.0 ± 1.2	68.6 ± 9.7	<0.001
Sex (male/female, n/n)	83/49	109/51	105/21	87/18	94/25	<0.001
Histology						
Intestinal type					87	
Diffuse type					32	
Clinical stage						
Stage I-II					80	
Stage III-IV					29	
CMA/B polymorphism						
G/G genotype	102 (77.3%)	114 (71.3%)	83 (65.4%	75 (71.4%)	67 (56.3%)	0.003
G/A genotype	27 (20.5%)	44 (27.5%)	36 (28.3%)	26 (24.8%)	45 (37.8%)	
A/A genotype	3 (2.2%)	2 (1.2%)	8 (6.3%)	4 (3.8%)	7 (5.9%)	
ACE polymorphism						
I/I genotype	50 (37.9%)	51 (31.9%)	50 (39.4%)	41 (39.0%)	54 (45.4%)	0.129
I/D genotype	60 (45.5%)	83 (51.9%)	63 (49.6%)	54 (51.4%)	53 (44.5%)	
D/D genotype	22 (16.6%)	26 (16.2%)	14 (11.0%)	10 (9.6%)	12 (10.1%)	

Data Analysis. Hardy-Weinberg equilibrium of allele frequencies at individual loci was assessed by comparing the observed and expected genotype frequencies using the χ^2 test. Differences in the *CMA/B* A/G and *ACE* I/D genotype/allele frequencies between the control and *H. pylori* infection–related disease groups were determined by the χ^2 test. Differences in serum levels of PG I and PG I/PG II ratios between different genotype groups were assessed by Student's *t* test. The effects of genotypes/alleles of *CMA* and *ACE* polymorphisms on the risk of gastric cancer development were expressed as odds ratios (OR) with 95% confidence intervals (CI) adjusted by age and sex. All *P* values were two-sided, and $P < 0.05$ were considered statistically significant.

Results

Characteristics of Enrolled Subjects. The mean age of subjects with gastric cancer was significantly higher than those of any other group ($P < 0.001$; Table 1). Then, the ORs for the development of gastric cancers, gastric ulcers, and duodenal ulcers were adjusted by sex, as well as age, as noted above.

***CMA/B* A/G and *ACE* I/D Polymorphisms and the Development of Gastric Cancers.** The genotype frequencies of the *CMA/B* A/G and *ACE* I/D polymorphisms in the *H. pylori*-negative control group did not deviate significantly from those expected under the Hardy-Weinberg equilibrium (Table 1).

In the *H. pylori*-negative subjects and in the *H. pylori*-positive gastritis alone group, the number of *CMA/B* A/A, A/G, and G/G genotypes and *ACE* I/I, I/D, and D/D genotypes were 3/27/102 and 50/60/27 in subjects without *H. pylori* infection and 2/44/116 and 51/83/26 in patients with gastritis alone, respectively, and no significant differences in the genotype frequencies of *CMA/B* and *ACE* polymorphisms among the two subgroups. Therefore, we combined patients from the *H. pylori*-negative group and *H. pylori*-positive gastritis alone group and used them as the control group for the gastric cancer and peptic ulcer cases in the present study.

The frequencies of the *CMA/B* A/A, A/G, and G/G genotype were 1.7%, 24.3%, and 74.0% in the control group, whereas those in the gastric cancer group were 5.9%, 37.8%, and 56.3%, respectively (Table 1). The adjusted ORs for gastric cancer risk in patients with A/A or A/G genotype of the *CMA/B* significantly increased (A/A genotype, adjusted OR, 7.115; 95% CI, 1.818-27.845; A/G genotype, adjusted OR, 1.956; 95% CI, 1.137-3.366, respectively) in comparison with those with the G/G genotype (Table 2). The adjusted OR of the carriage of the A allele was 2.219 (95% CI, 1.315-3.744), which was higher than non–A allele carriers (Table 2). When the gastric cancer group was classified into the intestinal type and diffuse type, the adjusted ORs of *CMA/B* G/A and A/A genotypes for intestinal type of gastric cancer were 1.899 (95% CI, 1.029-3.503) and 8.334 (95% CI, 1.832-37.906), respectively. The adjusted ORs of A allele carriers for intestinal type of gastric cancer were 2.181 (95% CI, 1.209-3.932) and 2.250 (95% CI, 1.025-4.943; Table 3).

The frequencies of the I/I, I/D, and D/D genotypes of the *ACE* were 34.6%, 49.0% and 16.4% in the control group, whereas those in the gastric cancer group were 45.4%, 44.5% and 10.1%, respectively (Table 1). There was no statistically significant difference in the frequencies of *ACE* genotypes between the gastric cancer group and the control group (Table 2). There were also no significant differences in the adjusted ORs of *ACE* genotypes with respect to the two different pathologic classifications and clinical stage of the gastric cancer group (Table 3).

***CMA/B* A/G and *ACE* I/D Polymorphisms and the Development of Peptic Ulcers.** The frequencies of the *CMA/B* A/A, A/G, and G/G genotype in the gastric ulcer and duodenal ulcer group were 6.3%, 28.3%, and 65.4%, and 3.8%, 24.8%, and 71.4%, respectively (Table 1). The adjusted ORs for gastric ulcer development in patients with the *CMA/B* A/A genotype significantly increased (adjusted OR, 3.450; 95% CI, 1.086-10.960) in comparison with those with the G/G genotype (Table 2). There was no association between duodenal ulcer development and *CMA/B* polymorphism. There was no statistically significant difference in the frequencies of *ACE* genotypes between the peptic ulcer group and the control group (Table 2).

Table 2. Influences of *CMA/B* and *ACE* genotypes on gastric cancer, gastric ulcer, and duodenal ulcer risks

	Gene		Adjusted OR (95% CI)	*P*
Gastric cancer	*CMA/B*	G/G	1.000 (ref)	
		G/A	1.956 (1.137-3.366)	0.015
		A/A	7.115 (1.818-27.845)	0.005
		A allele carriage	2.219 (1.315-3.744)	0.003
	ACE	I/I	1.000 (ref)	
		I/D	0.655 (0.384-1.117)	0.120
		D/D	0.439 (0.191-1.008)	0.052
		D allele carriage	0.625 (0.376-1.039)	0.070
Gastric ulcer	*CMA/B*	G/G	1.000 (ref)	
		G/A	1.283 (0.794-2.074)	0.309
		A/A	3.450 (1.086-10.960)	0.036
		A allele carriage	1.436 (0.911-2.266)	0.119
	ACE	I/I	1.000 (ref)	
		I/D	0.790 (0.497-1.255)	0.318
		D/D	0.592 (0.295-1.187)	0.140
		D allele carriage	0.739 (0.475-1.150)	0.180
Duodenal ulcer	*CMA/B*	G/G	1.000 (ref)	
		G/A	1.020 (0.601-1.730)	0.942
		A/A	1.784 (0.461-6.907)	0.402
		A allele carriage	1.070 (0.645-1.774)	0.794
	ACE	I/I	1.000 (ref)	
		I/D	0.795 (0.485-1.302)	0.362
		D/D	0.492 (0.255-1.079)	0.071
		D allele carriage	0.720 (0.449-1.155)	0.173

NOTE: ORs were adjusted by age and sex.

Combination of Allele Carriage of *CMA/B* and *ACE* Polymorphisms. The combination of allele carriage of *CMA/B* and *ACE* polymorphisms was classified into the four subgroups: G/I (combination of *CMA/B* G/G and *CMA* I/I genotype), G/D (*CMA/B* G/G and *CMA* I/D or D/D genotypes), A/I (*CMA/B* G/A or A/A and *CMA* I/I genotypes), and A/D (*CMA/B* G/A or A/A and *CMA* I/D or D/D genotypes). The adjusted ORs of the A/I combination group relative to the G/I combination group in gastric cancer patients was 4.749 (95% CI, 2.050-11.001; Table 4). However, G/D and A/D combinations of *CMA/B* and *ACE* polymorphisms had no significant effect on gastric cancer development (Table 4).

Characteristics of the Gastric Cancer Group by PG Assay in Relation to *CMA/B* and *ACE* Polymorphisms. In gastric cancer patients >50-years-old, the mean serum PG I level was 39.2 ± 4.1 ng/mL, which was significantly lower than those in the controls (70.2 ± 2.9 ng/mL, $P < 0.0001$). In all patients >50 years old, however, there were no significant differences in the mean serum PG I levels among different genotype groups of *CMA/B* and *ACE* polymorphisms ($P = 0.898$ and 0.554, respectively; Fig. 1A).

In gastric cancer patients >50-years-old, the mean serum PG I/PG II ratio was 2.6 ± 0.3, which was significantly lower than those in the controls (2.9 ± 0.1, $P = 0.011$). The mean serum PG I/PG II ratio in >50-year-old patients with the *CMA/B* G/G genotype was 4.1 ± 0.2, which significantly differed from those with the *CMA/B* A/G or A/A genotypes (3.5 ± 0.2, $P = 0.0388$; Fig. 1B). However, there were no significant differences in the mean serum PG I/PG II ratios among different allele carriages of *ACE* polymorphism ($P = 0.6142$; Fig. 1B).